

Appendix A

This Appendix explains the process of updating LANDFIRE vegetation geodata, calculating ecological departure, and simulating climate change effects using temporal multipliers in state-and-transition models.

Mapping Pre-settlement Vegetation and Current Vegetation

The foundation of ecological departure mapping is the stratification of a landscape via biophysical settings, or potential vegetation, as defined by LANDFIRE (www.landfire.gov; Rollins2009). Biophysical settings are conceptually similar to ecological sites from Natural Resource Conservation Service (NRCS) soil surveys, except the biophysical settings often represent groups of ecological sites dominated by the same upper-layer species. The NRCS defines ecological site as “a distinctive kind of land with specific physical characteristics that differs from other kinds on land in its ability to produce a distinctive kind and amount of vegetation.” (*National Forestry Manual*, www.nrcs.usda.gov/technical/ECS/forest/2002_nfm_complete.pdf).

For each biophysical setting (a.k.a. ecological system), current vegetation was also mapped as the natural succession classes and any uncharacteristic classes. Natural succession classes typically were based on the standard LANDFIRE model of up to five classes ranging from early- to mid- to late-development; mid- and late-development classes may be expressed as open or closed canopy. Uncharacteristic classes included the presence of uncharacteristic native species (e.g. loss of aspen regeneration, loss of aspen clones, encroachment of pinyon or juniper into shrublands and wet meadows, loss of the herbaceous understory of shrublands, and entrenchment and drop of the water table in riparian systems and wet meadows) and uncharacteristic exotic species (e.g., invasion of cheatgrass into shrublands and woodlands, and invasion of exotic forbs in wet meadows and riparian systems).

The LANDFIRE program has developed maps of biophysical settings and current vegetation succession classes for the entire United States (Rollins 2009). LANDFIRE’s remote sensing was based on multiple captures of Landsat imagery from the 1990s reflecting current land management practices. We clipped this GIS data to the ~5,000,000-acre project area. We refined the geodata using two major improvements: 1) replacing the LANDFIRE geodata covering National Forests with USFS’s enhanced biophysical settings and current vegetation classes and 2) remapping the LANDFIRE riparian layers with National Wetland Inventory (NWI) geodata.

- 1) National Forest geodata. After LANDFIRE made geodata available for download in 2009, Dr. Hugh Safford, the USFS regional ecologist for Region 5, used historic USFS vegetation plot data and maps to remap the LANDFIRE geodata for Region 5 National Forests, along with revising reference VDDT models and recalculating NRV. USFS used LANDFIRE’s definitions and standards. We used the new USFS geodata to replace the LANDFIRE geodata for approximately 70% of the study area (i.e., stamping new geodata over old geodata). The area outside National Forests was retained in their original LANDFIRE version.

- 2) Riparian geodata. LANDFIRE's biophysical setting map lacked Montane Wet Meadow, which is a critical ecological system for the Northern Sierra Partnership. LANDFIRE did not consider wet meadows as a distinct biophysical setting; therefore, they were not mapped. LANDFIRE mapped as agriculture (pasture), sagebrush, and riparian large areas we knew were large wet meadows. Without external geodata on wet meadows, it would not have been possible to map them. The NWI data were used to remedy biophysical setting shortcomings. Therefore, all NWI vegetation types that could be conceived as marsh, wet meadow, wetland, or naturally inundated lands were called montane wet meadow and replaced the LANDFIRE biophysical setting geodata. The new layer captured well known wet meadows. In a few very small cases, NWI mapped "forested coniferous swamp", which we lumped with lodgepole pine-wet (if LANDFIRE mapped forest types) or water (if LANDFIRE mapped water). The NWI geodata were limited to biophysical settings and could not provide any information for vegetation classes. The vegetation classes within each biophysical setting were obtained through a "coarse" crosswalk. Rules were:
- If wet meadow biophysical setting in LANDFIRE, then we made no change to vegetation classes;
 - If sagebrush biophysical setting in LANDFIRE, then we changed the area to wet meadow class U (Uncharacteristic) *Desertification* (lowered water table or diverted water favoring subxeric shrubs);
 - If forest (usually conifers) biophysical setting in LANDFIRE, then we changed the area to wet meadow class U *Tree-Encroached* (conifer encroachment for usually lowered water table or diverted water);
 - If agriculture or pasture in LANDFIRE, then we changed the area to wet meadow class C *late-succession*.

Evaluating Current Ecological Condition

We assessed the condition of each major ecological system by mapping ecological departure (a.k.a., Fire Regime Condition or FRC) using the methodology developed under the U.S. interagency LANDFIRE program (Hann and Bunnell, 2001; Shlisky and Hann 2003; Rollins 2009; and adapted by Provencher et al. 2008). The fundamental elements of ecological departure analysis include mapping the distribution of ecological systems that existed prior to European settlement or are today naturally functioning, mapping current vegetation and succession classes, and calculating dissimilarity between current and pre-settlement (or naturally functioning) conditions. Ecological departure is an integrated, landscape-level measure of ecological condition that incorporates species composition, vegetation structure, and all significant disturbances (not only fire) for terrestrial and riparian ecological systems that would have occurred pre-settlement or in naturally functioning landscapes. This methodology determines the dissimilarity between an ecological system's current (or future simulated) condition and its natural range of variability (NRV). NRV reflects the distribution of vegetation classes that would be found under naturally functioning ecological processes, as predicted by field studies, expert opinion, and computer simulations. We calculated the ecological departure of each ecological system from new NRV using the grid data obtained from LANDFIRE, USFS geodata,

and NWI. Ecological departure is scored on a scale of 0% to 100% departure from NRV using the standard LANDFIRE methodology: 0% represents NRV while 100% represents total departure from NRV (dissimilarity equation in Provencher et al. 2008).

Assessing Future Condition

Predictive Ecological Models

In order to forecast future condition with and without projected climate change effects (as well as to test alternative conservation strategies), one state-and-transition model was developed for each biophysical setting using Vegetation Dynamics Development tool (VDDT; Barrett 2001; Beukema et al. 2003) software. A state-and-transition model is a discrete, box-and-arrow representation of the continuous variation in vegetation composition and structure of an ecological system (Bestelmeyer et al., 2004). Different boxes either belong to different *phases* within a state or different *states*. States are formally defined in rangeland literature (Bestelmeyer et al., 2004) as: persistent vegetation and soil changes per potential ecological sites that can be represented in a diagram with two or more boxes (phases of the same state). Different states are separated by “thresholds.” A threshold implies that substantial management action would be required to restore ecosystem structure and function. Relatively reversible changes (e.g., fire, flooding, drought, insect outbreaks, and others), unlike thresholds, operate between phases within a state. All ecological system models had at their core the LANDFIRE reference condition represented by some variation around the A-B-C-D-E succession classes, which are phases within the reference state. (Some USFS models had an F class representing an alternative early succession class.) The A-E class models typically represent succession from usually herbaceous vegetation (class A) to increasing woody species dominance where the dominant woody vegetation might be shrubs (class C) or trees (class E).

We used LANDFIRE-based descriptions and models as modified by Dr. Hugh Safford for the five predominant forest systems in the Sierra Nevada. For other systems, we used LANDFIRE descriptions and models or descriptions and models applied in the Bodie Hills in eastern California (Provencher et al., 2009; Low et al, 2010).

The models for many ecological systems included “uncharacteristic” (U) classes. Uncharacteristic classes are classes outside of reference conditions. Ecological departure calculations do not differentiate among the uncharacteristic classes – i.e., all U-classes are treated as equally outside of NRV. However, the cost and management urgency to restore different uncharacteristic classes varies greatly. TNC therefore previously developed and applied a separate designation and calculation of “high-risk” vegetation classes. A high-risk class was defined as an uncharacteristic vegetation class that met at least one out of three criteria: 1) $\geq 5\%$ cover of invasive non-native species, 2) very expensive to restore, or 3) a direct pathway to one of these classes (invaded or very expensive to restore) (Low et al., 2010). We secured rates of conversion to uncharacteristic classes (e.g. the rate of cheatgrass invasion for ponderosa and Jeffrey pines) based on expert opinion and observational data (*personal communication*, Dr. Kyle Merriam, Plumas National Forest).

Accounting for Variability in Disturbances

The basic VDDT models incorporate stochastic disturbance rates that vary around a mean value for a particular disturbance associated with each ecological system. The default variability is relatively minor in magnitude. For example, fire is a major disturbance factor for most of the Northern Sierra's ecological systems, including replacement fire, mixed severity fire, and surface fire. These fire regimes have different rates or probabilities of occurrence in a given year (i.e., inverse of the mean fire return interval) that are incorporated into the models for each ecological system where they are relevant. However, in real-world conditions the disturbance rates are likely to vary appreciably over time. To simulate strong yearly variability for fire activity, drought-induced mortality, non-native species invasion rates, tree encroachment rate, loss of herbaceous understory, flooding, and so on, TNC incorporated temporal multipliers in the model run replicates. This approach was pioneered by TNC for the Bodie Hills project at the request of the Bureau of Land Management Bishop Field Office (Provencher et al., 2009).

A temporal multiplier is a number in a yearly time series that multiplies a base disturbance rate in the VDDT models: e.g., for a given year, a temporal multiplier of one implies no change in a disturbance rate, whereas a multiplier of zero is a complete suppression of the disturbance rate, and a multiplier of three triples the disturbance rate. A temporal multiplier can be obtained from time series data or theoretically derived.

We generated temporal multipliers for two different purposes: 1) to represent the reference condition and estimate new NRV (i.e., we did not use NRV provided by LANDFIRE) and 2) to represent the period of fire suppression and land management in the northern Sierra Nevada.

NRV Estimation. The Palmer Drought Severity Index (PDSI) was used to create most temporal multipliers, including for fire. The PDSI (mean monthly November-April; raw numbers were not modified) for the region was used to create 100-year temporal multipliers to more accurately reflect annual variability in fire and other disturbance regimes. The PDSI period from 1896-2006 was obtained from the USFS (also: Data source from NOAA National Climate Data Center - <http://www.ncdc.noaa.gov/oa/mpp/>). Taylor and Beaty (2005) showed that the PDSI is highly negatively correlated to fire frequency and total area burned for forest types during pre-settlement: more fire was observed during increasingly drier years. The same relationship holds for average temperature (Westerling et al. 2006). This, however, does not apply to shrublands that must first experience consecutive wetter than average years to accumulate fine fuels that will more likely burn in a dry year immediately following the wet year sequence (Westerling and Bryant 2008; Westerling, *in press*). The first replicate of the PDSI time series was obtained from the 1896 to 1995 period. The next four replicates were randomly resampled with replacement from the full 111-year time series with MS Excel's VLOOKUP function; they conserved the original time series' number of high and lows, and magnitude of area burned per year. Cyclical behavior, such as caused by climate forcing factors, will not be preserved by this approach.

By trial-and-error, we fitted equations that converted the PDSI time series values into temporal multipliers of fire and other mortality sources that had to satisfy one important condition: the results of NRV simulations with their imbedded temporal multipliers had to reproduce USFS data-supported estimated fire and insect/disease rates (probability per year) when simulated to equilibrium in each of five VDDT major forest model developed by

Safford. In other words, fire and insect/disease rates in the VDDT models were “true” because USFS staff had estimated them from field data, whereas the PDSI variability we were introducing as an external forcing factor had never been used for simulations. Therefore, simulations with PDSI had to yield realized rates for fire and insect/disease that approximately equaled the field estimates, which in turn required transformation of the yearly PDSI values for each temporal multiplier series. Different negative exponential equations were used because the general form of the negative exponential appropriately damped the effects of wet and average years (positive PDSI) but magnified the effects of truly dry years (negative PDSI) (Table A-1; Figure A-1 except intraspecific competition). Obtaining the best fitting negative exponential equation for each simulation type was an incremental trial-and-error process in parameter fitting. Using temporal multipliers from Table A-1, simulations were run for 100 years to obtain equilibrium values for vegetation classes. If equilibrium was not achieved after 100 years, the previous run’s end values became the initial conditions for the next 100 years and repeated until equilibrium was reached. Equilibrium values were the NRV.

Table A-1. Temporal multipliers fitting equations for biophysical settings developed by USFS R5. Legend: RF = replacement fire, MF = mixed severity Fire, SF = surface fire, and I/D = insect & disease.

Biophysical setting	RF	MF	SF	I/D	Intra-specific Competition [#]
Red Fir-White Pine	$0.5474e^{-0.4938\text{PDSI}}$	$0.0364e^{-1.5\text{PDSI}}$	$0.5202e^{-0.7177\text{PDSI}}$	$0.5474e^{-0.4938\text{PDSI}}$	
Red Fir-White Fir	$0.5474e^{-0.4938\text{PDSI}}$	$0.0364e^{-1.5\text{PDSI}}$	$0.5202e^{-0.7177\text{PDSI}}$	$0.194e^{-0.8056\text{PDSI}}$	
Mixed Conifer	$0.5474e^{-0.4938\text{PDSI}}$	$0.0364e^{-1.5\text{PDSI}}$	$0.5652e^{-0.5664\text{PDSI}}$	$0.5474e^{-0.4938\text{PDSI}}$	$\frac{e^{-\text{PDSI} + \text{abs}(\min[\text{PDSI}, 1])}}{e^{-\text{abs}(\min[\text{PDSI}, 1])}}$
Ponderosa Pine	$0.5474e^{-0.4938\text{PDSI}}$	$0.0364e^{-1.5\text{PDSI}}$	$0.5202e^{-0.7177\text{PDSI}}$	$0.5652e^{-0.5664\text{PDSI}}$	$\frac{e^{-\text{PDSI} + \text{abs}(\min[\text{PDSI}, 1])}}{e^{-\text{abs}(\min[\text{PDSI}, 1])}}$
Jeffrey Pine	$0.5474e^{-0.4938\text{PDSI}}$	$0.194e^{-0.8056\text{PDSI}}$	$0.5652e^{-0.5664\text{PDSI}}$	$0.5652e^{-0.5664\text{PDSI}}$	$\frac{e^{-\text{PDSI} + \text{abs}(\min[\text{PDSI}, 1])}}{e^{-\text{abs}(\min[\text{PDSI}, 1])}}$

[#]Intra-specific competition among early-succession saplings was included in USFS models, but a field-estimated was not provided; therefore, we could not fit an equation. We developed a plausible equation that caused wetter than average years to suppress intra-specific competition.

Temporal Multipliers for Estimating NRV

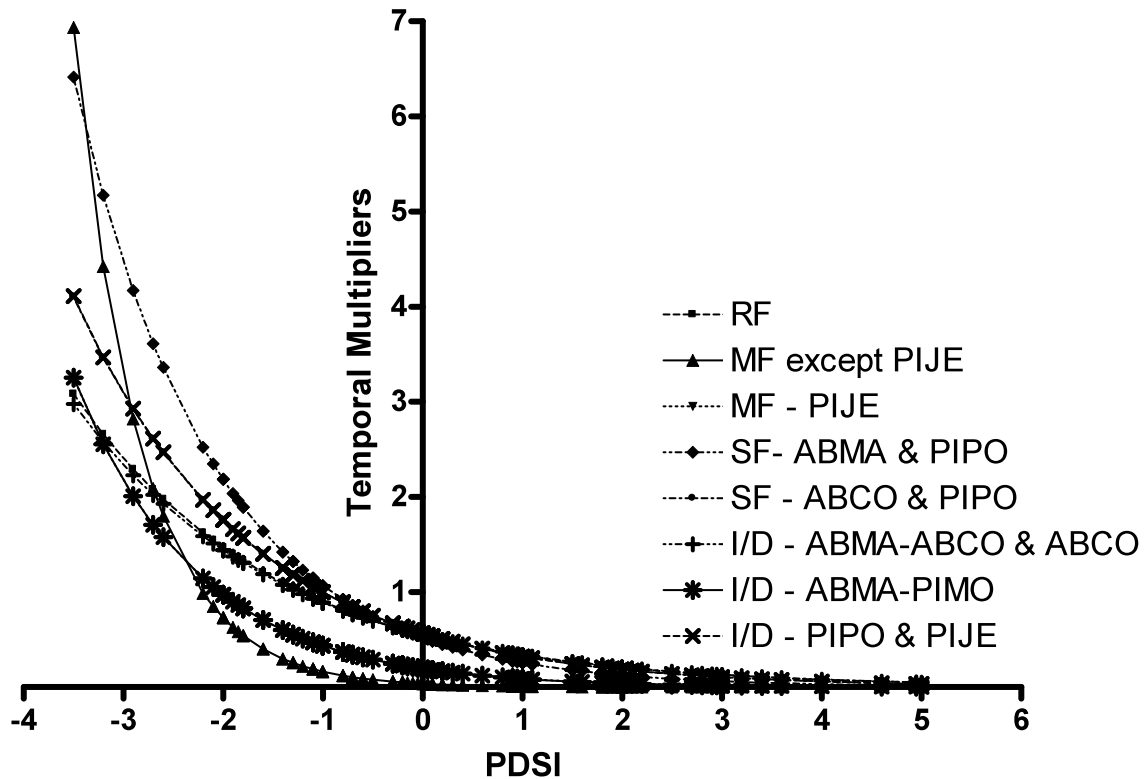


Figure A-1. Temporal multipliers based on the Palmer Drought Severity Index (PDSI) for biophysical settings developed by USFS R5. Legend: RF = replacement fire, MF = mixed severity Fire, SF = surface fire, and I/D = insect & disease, PIJE = Jeffrey pine, ABMA = California red fir, PIPO = ponderosa pine, ABCO = white fir, and PIMO = western white pine.

Temporal multiplier equations in Table A-1 applied to Safford’s five models. There were, however, 20 other biophysical settings that also needed temporal multipliers based on PDSI for consistency in methods. “Thematic” temporal multipliers were developed by which similar biophysical settings were grouped: i) shrublands - subxeric woodlands, ii) alpine – subalpine – wet systems (including aspen), and iii) low- and mid-elevation forests. These are shown in Table A-2. The low- and mid-elevation forest group essentially shared ponderosa pine’s temporal multipliers. The shrubland - subxeric woodland group was based on our work in the Bodie Hills of eastern California for big sagebrush (Provencher et al., 2009). The temporal multiplier equation for fire in shrublands reflects the fact that moisture and fine fuels have to build up with above average moisture before fire can spread in these subxeric systems (Westerling, *in press*): it is the only equation that considers PDSI over two consecutive years. The alpine-subalpine-wet system group included all systems that are not water limited, except during droughts.

Table A-2. Temporal multiplier fitting equations for biophysical settings not developed by USFS R5. Legend: RF = replacement fire, MF = mixed severity Fire, SF = surface fire, and I/D = insect & disease.

Biophysical setting	RF	MF	SF	I/D	Drought	Snow-Deposition	Very-Wet-Year
Alpine-Subalpine-Wet Systems (including Aspen)	$0.5474 \times e^{-0.4938PDSI}$	$0.0364 \times e^{-1.5PDSI}$		$0.5474 \times e^{-0.4938PDSI}$	$0.5474 \times e^{-0.4938PDSI}$	if(PDSI < -2.5 then =0 else =0.9334 + 0.3338PDSI)	
Low & Mid-Elevation Forest	$0.5474 \times e^{-0.4938PDSI}$	$0.0364 \times e^{-1.5PDSI}$	$0.5652 \times e^{-0.5664PDSI}$	$0.5652 \times e^{-0.5664PDSI}$			
Shrubland-Subxeric Woodland	$e^{0.5(PDSI_t - PDSI_{t+1})} \times e^{-0.1PDSI_{t+1}}$		$e^{0.5(PDSI_t - PDSI_{t+1})} \times e^{-0.1PDSI_{t+1}}$		$0.5474 \times e^{-0.4938PDSI}$		If(PDSI > 2, then =PDSI else =0)

Temporal multipliers for montane-subalpine riparian systems (not shown in Table A-2) were strongly dependent on flow variations (Rood et al., 2003; McBride and Strahan, 1984). We had recently developed long term flow temporal multipliers for the lower Truckee River (USGS Sparks Truckee River gage), which is highly influenced by the Pacific Ocean and representative of the whole northern Sierra Nevada. Variability of the 7-year, 20-year, and 100-year flood events used in the models were all based on filtering the full time series for increasingly higher values of annual peak flow that correspond to these flood events. The three levels of flooding corresponded to 7-year events that killed or removed only herbaceous vegetation; 20-year events that killed or removed shrubs and young trees; and 100-year events that top-killed larger trees (i.e., these are three distinct disturbances in the riparian VDDT models). All temporal multipliers were obtained by dividing peak flow from each year by the temporal average of peak flow. Based on known flood events for the Truckee River, the 7-year, 20-year and 100-year flood events, respectively, corresponded to ~0.8, ~1 and ~3.69 of the flood temporal multiplier series: All values less, respectively, than the thresholds of 1 and 3.69 for the 20-year and 100-year flood events were zero because they did not have enough force to destroy class-dependent vegetation (i.e., had no effect on vegetation in the class), whereas all values above the flood event thresholds were used directly as a temporal multiplier (Figure A-2). The 7-year flood events encompass the full time series of peak flow because few peak flows were below the 7-year event threshold and those that were below actually suppressed the model's disturbance rate.

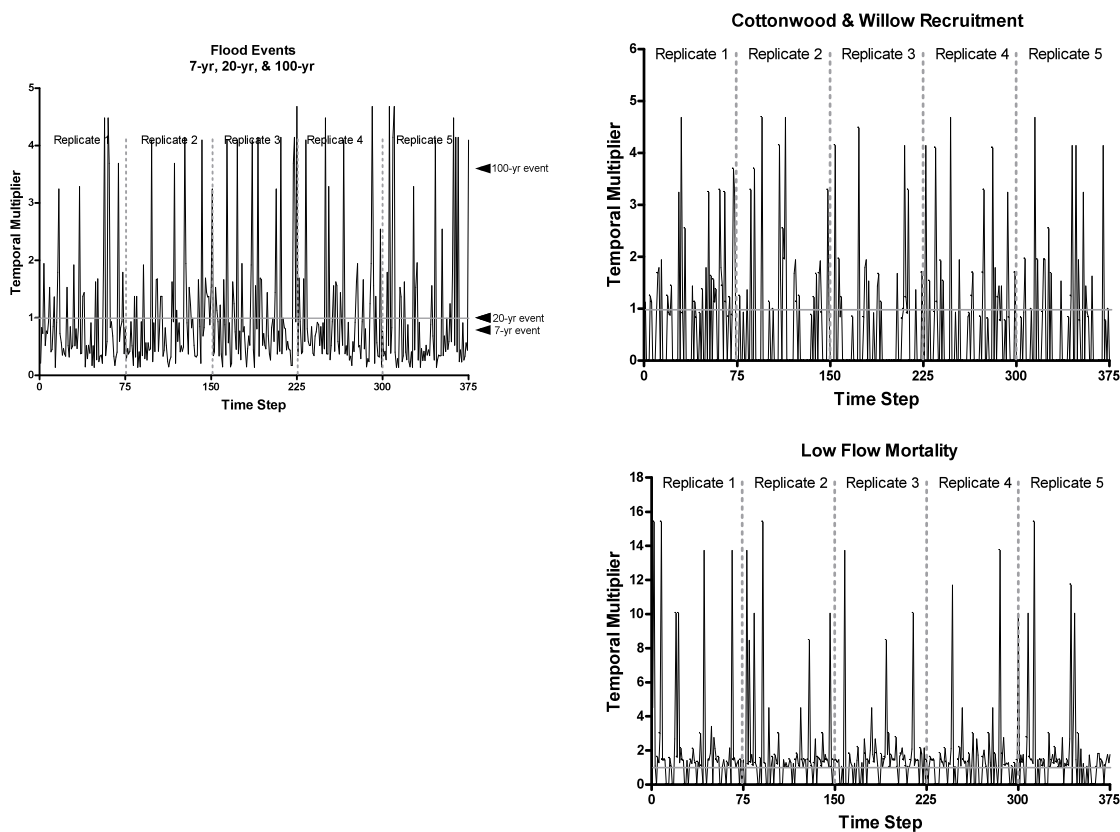


Figure A-2. Riparian temporal multipliers a) for 7-year, 20-year, and 100-year flood events, b) for cottonwood and willow recruitment, and c) for low average August and September flows that kill cottonwood and willow seedlings. For the 20-year and 100-year flood events, respectively, all values below their threshold were zero. Data obtained from the Sparks Truckee River U.S. Geological Survey gage. The gray line for temporal multiplier = 1 represented the “no-change” or neutral parameter line.

Two other riparian disturbances were used during the first two years of succession: *cottonwood-willow recruitment* and *low-flow-kill*. Each had a temporal multiplier based on different flow data. *Cottonwood-willow recruitment* depends on flood stage and recession rate (Rood et al., 2003; McBride and Strahan, 1984), which do not translate nicely into the yearly time step of VDDT models. To imitate the effect of stage and recession on *Cottonwood-willow recruitment*, two dependent components that had to be met for successful recruitment:

1. Recruitment was more successful as peak flows increased in a given year for various reasons, including scouring and creation of wetted mineral surface. The temporal multiplier (yearly peak flow divided by the temporal average of peak flow) contributed to recruitment if it was > 0.77 or a 5-year flood event, which is a typical minimum overbank flow value; (Figure A-2); and

2. Given peak flows were sufficient for recruitment, sometimes recruitment failed for purely random reasons in a year due to various factors including the shape of the hydrograph (appropriate recession rate) and weather. We assigned an arbitrary 5% rate of failure of cottonwood and willow germination (i.e., 95% of times germination would succeed). The 5% rate of failure to germinate was randomly drawn from a uniform distribution in MS Excel (RAND() function).

After recession of spring flows, low-flow-kill was a source of mortality applied to the established cottonwood and willow seedlings (i.e., successfully germinated in June and July) that was caused by desiccation of seedlings from prolonged lower summer flows. The lowest water months of the year causing this mortality were August and September. We summed August and September flows in a year and then divided them by the temporal average of this sum to obtain the temporal multiplier time series. If the low-flow temporal multiplier was >1 (i.e., more water than average), *low-flow-kill* was zero (i.e., no desiccation), otherwise *low-flow-kill* was the inverse of the low flow temporal multiplier (i.e., greater mortality for lower summer flows; Figure A-2).

We used PDSI to calculate NRV because PDSI captured the high variability of dry and wet years, and fire activity in the northern Sierra Nevada (Taylor and Beaty 2005). However, we do not necessarily recommend the approach of incorporating more realistic levels of variability to estimate NRV as a general practice for other projects because significant changes in the PDSI or any critical time series data (spatially or duration) can lead to a different recalibration of the models parameters and NRV. Our approach was very time-consuming. The accepted standard method for NRV estimation — LANDFIRE's — does not use any external source of variability (i.e., no temporal multipliers) other than the default variability of VDDT and is far less arduous.

Incorporating Fire and Land Management into Models. Different fire temporal multipliers were used for post-settlement models than for NRV models. We secured fire history geodata for the northern Sierra Nevada from federal and state sources to more accurately reflect the actual annual variability in fire activity in the forest ecosystems during the XXth century and early XXIst century — including fire suppression and wildfires escaping suppression efforts. The temporal multipliers used for this phase of modeling were based on total area burned geodata from federal, state, and private lands over ~107 years. Three steps were involved:

1. Partition area burned: Using GIS, we clipped the fire area geodata to the east and west sides of the Sierra Nevada, and further separated those areas by biophysical settings, to create 100-year (the full time series was 107 years long) fire time series per biophysical setting.
2. Sum area burned by major biophysical setting groups: The area burned by biophysical setting was pooled (summed) into five major functional groups and fire temporal multipliers (area burned in a year divided by the temporal average of area burned) were calculated for these groups to avoid tedious and possibly sized-bias temporal multiplier calculations, especially for small systems (Table A-3).

3. Partition by fire severity: Total are burned by major biophysical setting group was partitioned among the three fire severity types (replacement = high, mixed = intermediate, and surface = low); otherwise the variability of replacement fire would equal that of surface fire and lead to intense and unrealistic fire activity in forests and rangelands that are currently fire suppressed. To obtain the severity type proportions, VDDT models of the most dominant biophysical settings were inventoried for their realized disturbance rates (result of simulations). We then averaged these rates across biophysical settings by fire type. These rates were divided by their total (of the three types) to guarantee a total proportion of one (Table A-4). As a final result, fifteen time series (i.e., three time series per each of five replicates, one each for replacement, mixed severity, and surface fire) were uploaded into the appropriate VDDT models, and yearly probability multiplier values multiplied the average wildfire rate in the models. All replicates had differing peaks and lows of fire activity. Importantly, the temporal multipliers reflected fire suppression practices and human activity of the last century and were considered the “no-climate change” version for all simulations.

Table A-3. Biophysical settings by functional groups.

Functional Group	Biophysical Setting
Alpine & Subalpine	<ul style="list-style-type: none"> Subalpine meadow Alpine Shrubland Lodgepole Pine-dry Lodgepole Pine-wet Subalpine Woodland Red Fir-Western White Pine Red Fir-White Fir
Mid-Elevation Forest	<ul style="list-style-type: none"> Mixed Conifer-Mesic Yellow Pine East Side Ponderosa Pine-Mixed Conifer California Oak-Pine Forest Wet Meadow California Montane Riparian Great Basin Montane Riparian
Mid-Elevation Eastern Shrubland	<ul style="list-style-type: none"> Montane sagebrush Steppe Big Sagebrush Shrubland Low Sagebrush Pinyon-Juniper Woodland Curleaf Mountain Mahogany

	Aspen Woodland Aspen-Mixed Conifer Forest
Xeric-Shrubland	
	Ultramafic Woodland and Chaparral Montane Chaparral
Lower-Elevation-Western Forest & Woodland	
	California Mixed Evergreen Forest Blue Oak-Pine Foothill Woodland

Table A-4. Relative proportions of fire severity types.

Functional Group	Fire Type	Relative Proportion
Alpine & Subalpine		
	surface fire	0.73
	mixed fire	0.19
	replacement fire	0.07
Mid-Elevation Forest		
	surface fire	0.35
	mixed fire	0.39
	replacement fire	0.26
Mid-Elevation Eastern Shrubland ^{&}		
	surface fire	0.01
	mixed fire	0.01
	replacement fire	0.98
Xeric-Shrubland ^{&}		
	surface fire	0.01
	mixed fire	0.01
	replacement fire	0.98
Lower-Elevation Western Forest & Woodland [#]		
	surface fire	0.35
	mixed fire	0.46
	replacement fire	0.19

[&] These types generally only have replacement fire; however 1% each for mixed severity and surface fire were allowed for a few exceptions.

[#] Based on ponderosa pine VDDT data

Temporal multipliers for drought-induced mortality, insects and disease, snow deposition, very-wet-year, flooding, cottonwood-willow-recruitment, and low-flow-kill that were shown above for NRV estimation were also used in management models. The Truckee River flow temporal multipliers were kept to represent the east side; however, new USGS gage data were obtained from the Feather River at Oroville to calculate west side 7-, 20-, and 100-year flood events, cottonwood-willow recruitment, and low-flow-kill temporal multipliers.

New temporal multipliers were needed, however, for tree (singleleaf pinyon and Utah or western juniper) encroachment into shrublands and non-native species invasions. We assumed that the rate of annual grass-invasion was greatest in wetter years and least in drier years (Table A-5). Tree encroachment similarly responded to PDSI, but we assumed a much slower process (Table A-5). Both temporal multiplier equations were linear for the non-null portion of the relationship. Linearity was chosen as the simplest assumption because Dr. Robert Nowak at University of Nevada, Reno indicated that he was not aware of any published data to inform our pixel-based modeling.

Table A-5. Temporal multipliers fitting equations by biophysical setting. Legend: AG-Invasion = annual-grass invasion.

Biophysical setting	Tree-Invasion	AG-Invasion
Ponderosa Pine & Jeffrey Pine		$f(\text{PDSI} < -2.5 \text{ then } 0 \text{ else } 1.8 + 0.7156\text{PDSI})$
Sagebrush, Pinyon-Juniper & Mountain Mahogany Woodland	$\text{if}(\text{PDSI} < -2.5 \text{ then } 0 \text{ else } 0.9334 + 0.3338\text{PDSI})$	$\text{if}(\text{PDSI} < -2.5 \text{ then } 0 \text{ else } 1.8 + 0.7156\text{PDSI})$

A final parameter was exotic forb-invasion in montane-subalpine riparian and wet meadow. We assumed that years of greater average annual flows would favor the invasion of exotic forbs. The exotic forb invasion temporal multiplier was the only one based on average annual flow because we assumed that year-round flows provided the soil moisture to promote weed growth. The rate of exotic forb invasion was, therefore, multiplied by the annual flow temporal multiplier (Figure A-3).

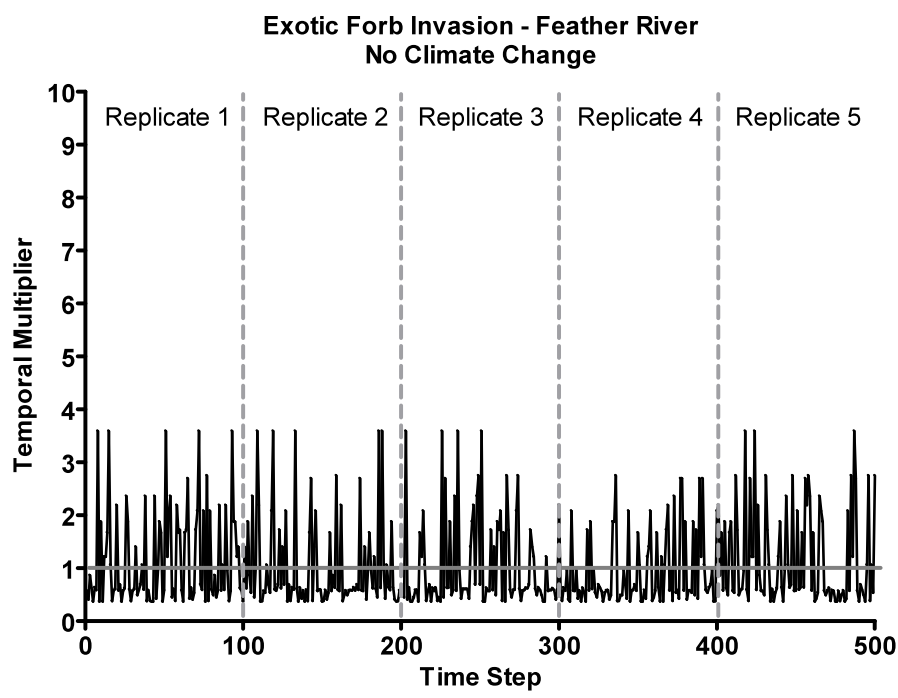
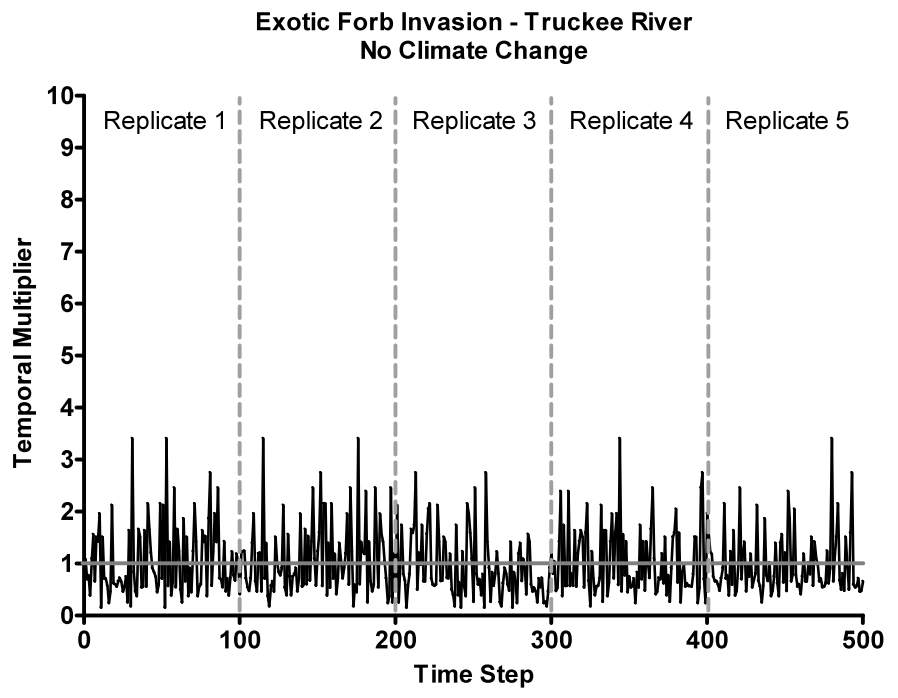


Figure A-3. Temporal multipliers for exotic fob invasion for the Truckee River (east side, upper graph) and Feather River (west side; lower graph). Under the no-climate change scenario, the exotic forb invasion temporal multiplier is equal to the annual flow temporal multiplier. The y-axis was set high to facilitate the comparison to the climate change scenario presented below.

Modifications of Temporal Multipliers to Reflect Future Climate Change

Fire Temporal Multipliers

We modified several replicate temporal multipliers from the east and west sides to simulate future fires assuming increasingly higher temperatures and about the same total precipitation (Parallel Climate Model with the business-as-usual B066.44 scenario from Dettinger et al., 2004; Figure A-4), and increasing green house gases (Figure A-4; IPCC 2007). The temperature, precipitation, and GHG multipliers were calculated differently than other temporal multipliers (the precipitation temporal was not needed): The temperature and GHG temporal multiplier time series were, respectively, obtained by dividing each year's value (in degree Celsius for temperature) by the value of temperature and GHG of the first year of the time series. We chose this different calculation of temporal multipliers under the assumption of increasing temperature and GHG would increasingly affect model parameters and that the beginning of the simulation is not affected by climate change factors (thus, temporal multiplier of the first year = 1). In retrospect, however, we recommend the standard division by the time series' temporal average to minimize, but not remove problems with unit conversions (e.g., Fahrenheit versus Celsius), but then adding a constant to all transformed values such that the first temporal multiplier at the beginning of the series is equal to one.

The simplest, most generic modification of historic fire temporal multiplier was to multiply year for year each historic replicate fire temporal multiplier for each of the five vegetation groups by the predicted temperature temporal multiplier (Figure A-4). This assumed that higher temperature caused more forest fire activity in a linear manner. The assumption of higher temperature or greater PDSI causing more fire activity is highly supported for forested systems (Taylor and Beaty 2005; Westerling et al. 2006; Westerling and Bryant 2008; Westerling *in press*). Westerling and Bryant (2008) showed nonlinearities between area burned and maximum temperature; however, their predictions under the A2 emissions scenario showed a nearly linear relationship between percent change in number of voxels (i.e., unit of lat × long × month) burned with fires >200 ha and future years of simulation. This bulk update of future fire activity resulted in 15 new temporal multipliers (5 groups × 3 fire severities) for each of the east and west sides representing climate change.

Temporal multipliers for fire, with and without climate change, are depicted in Figures A-5 to A-14. Every 100-year segment of the x-axis is a replicate.

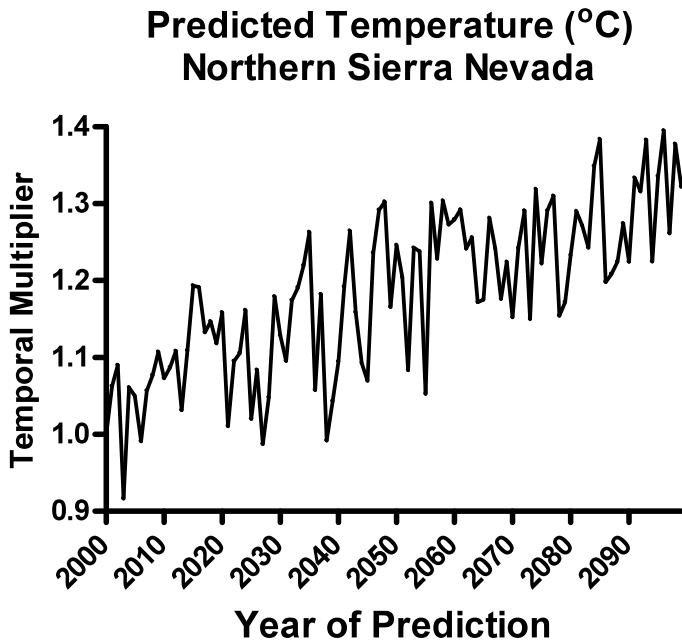
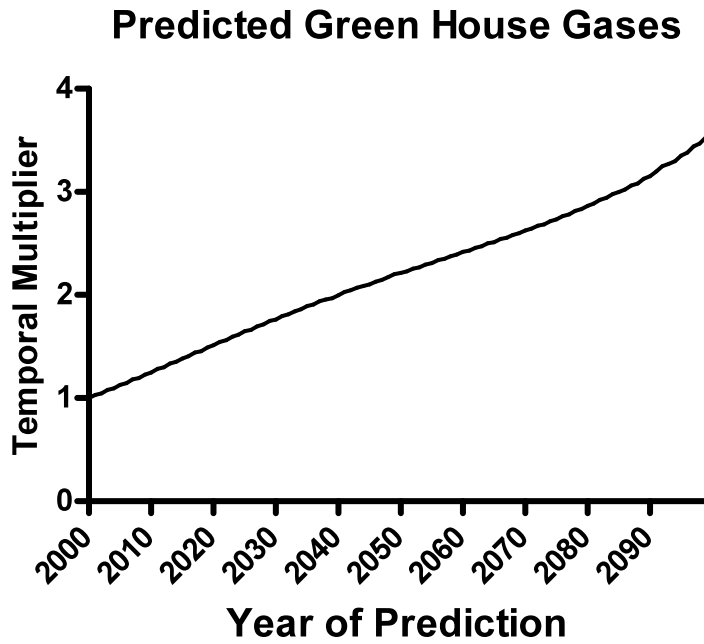


Figure A-4. Temporal multiplier of temperature for the Northern Sierra Nevada (based on Dettinger et al. 2004) and global green house gases (based on IPCC 2007) under the “business-as-usual” (A2) climate change scenario. Temperature raw data obtained from Dr. M. Dettinger, USGS, 2009 based on the PCM simulations. The green house gases and temperature temporal multipliers were each calculated by dividing each yearly value by the value of the first year of the time series.

East Side - Low-Elevation Forest Fire Multipliers

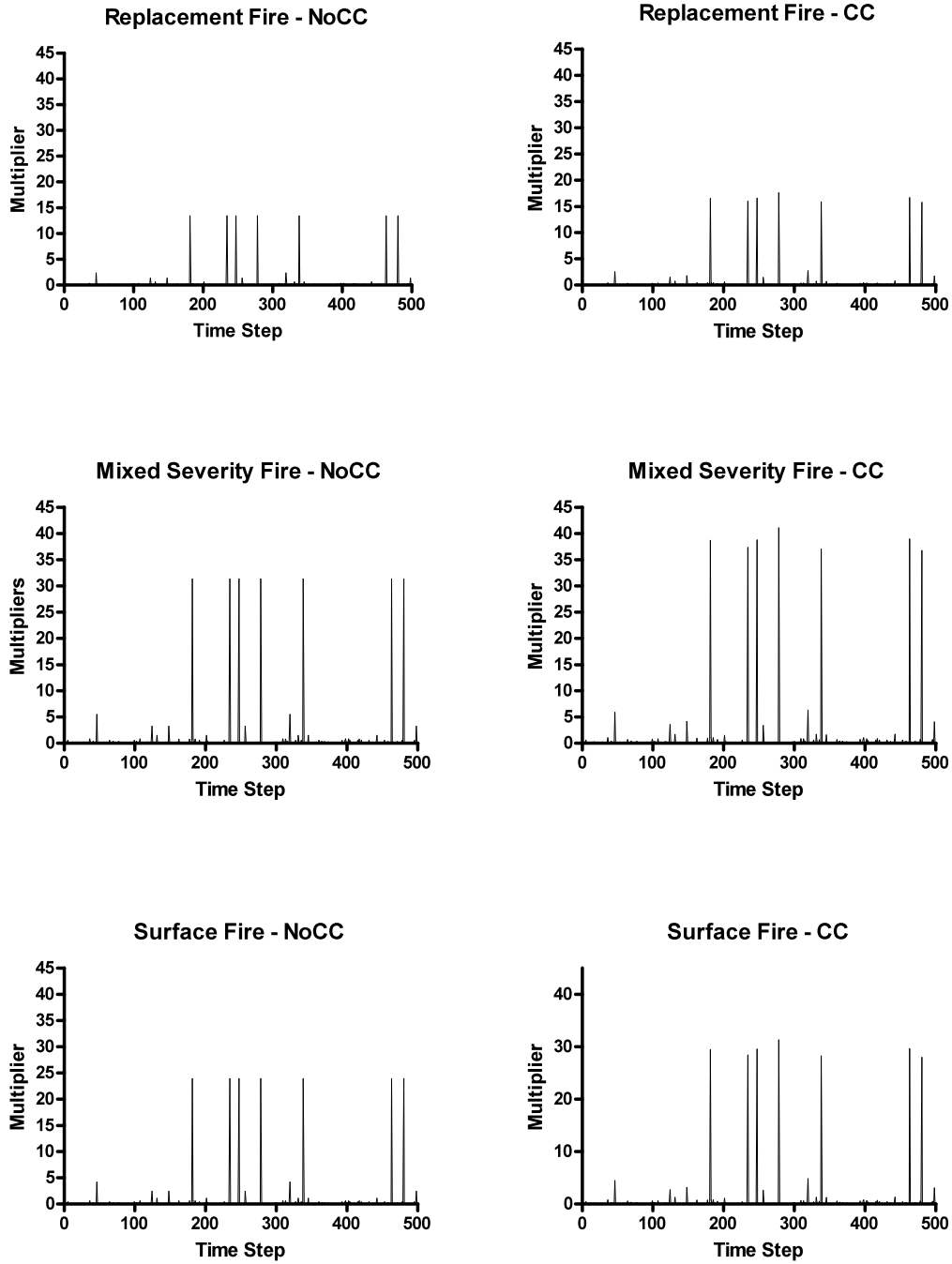


Figure A-5. Temporal multipliers of fire severity types for low elevation forest types on the east side of the Sierra Nevada.

East Side - Mid-Elevation Forest & Meadow Fire Multipliers

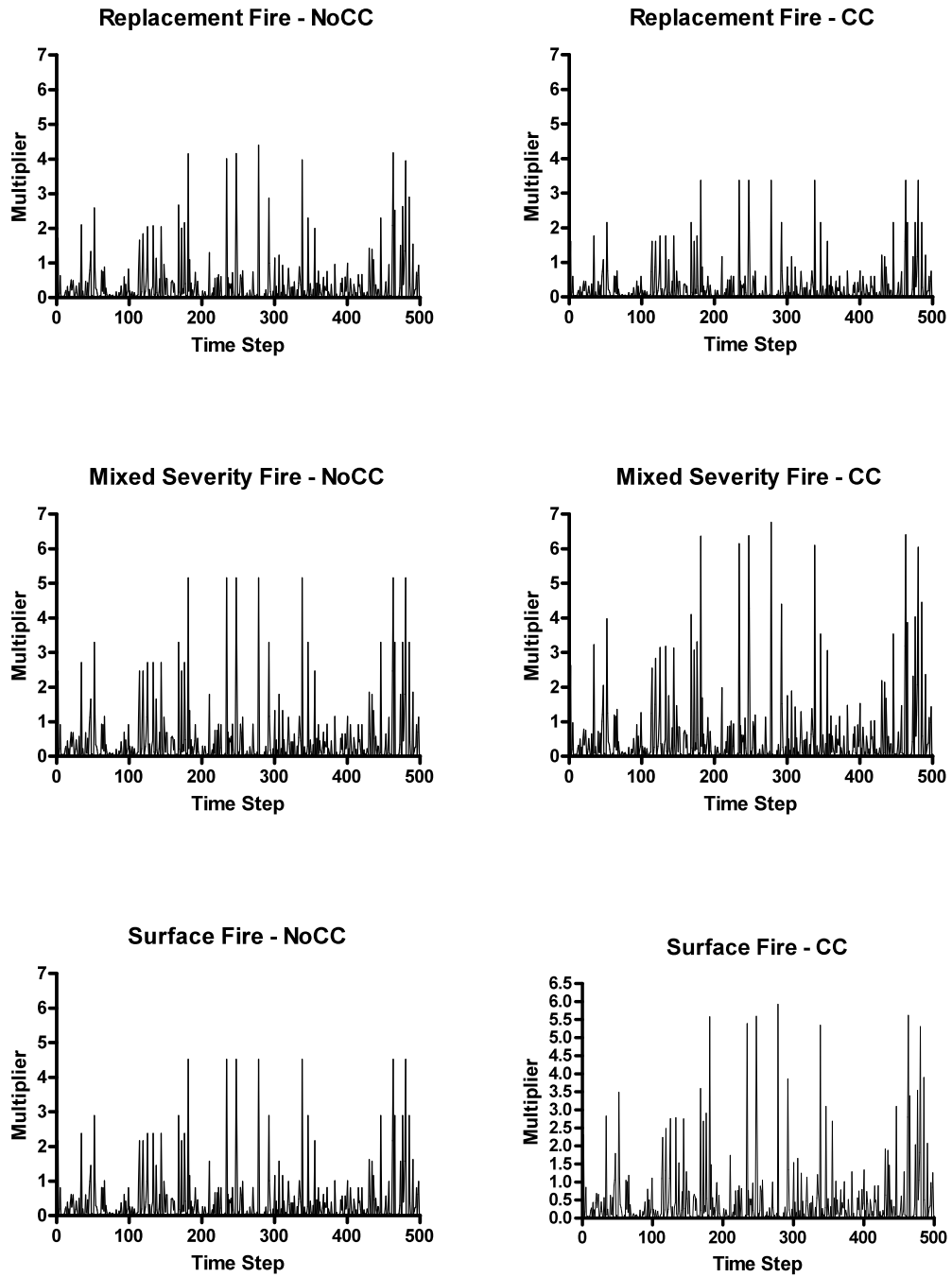


Figure A-6. Temporal multipliers of fire severity types for mid- elevation forest types on the east side of the Sierra Nevada.

East Side - Subalpine Forest Fire Multipliers

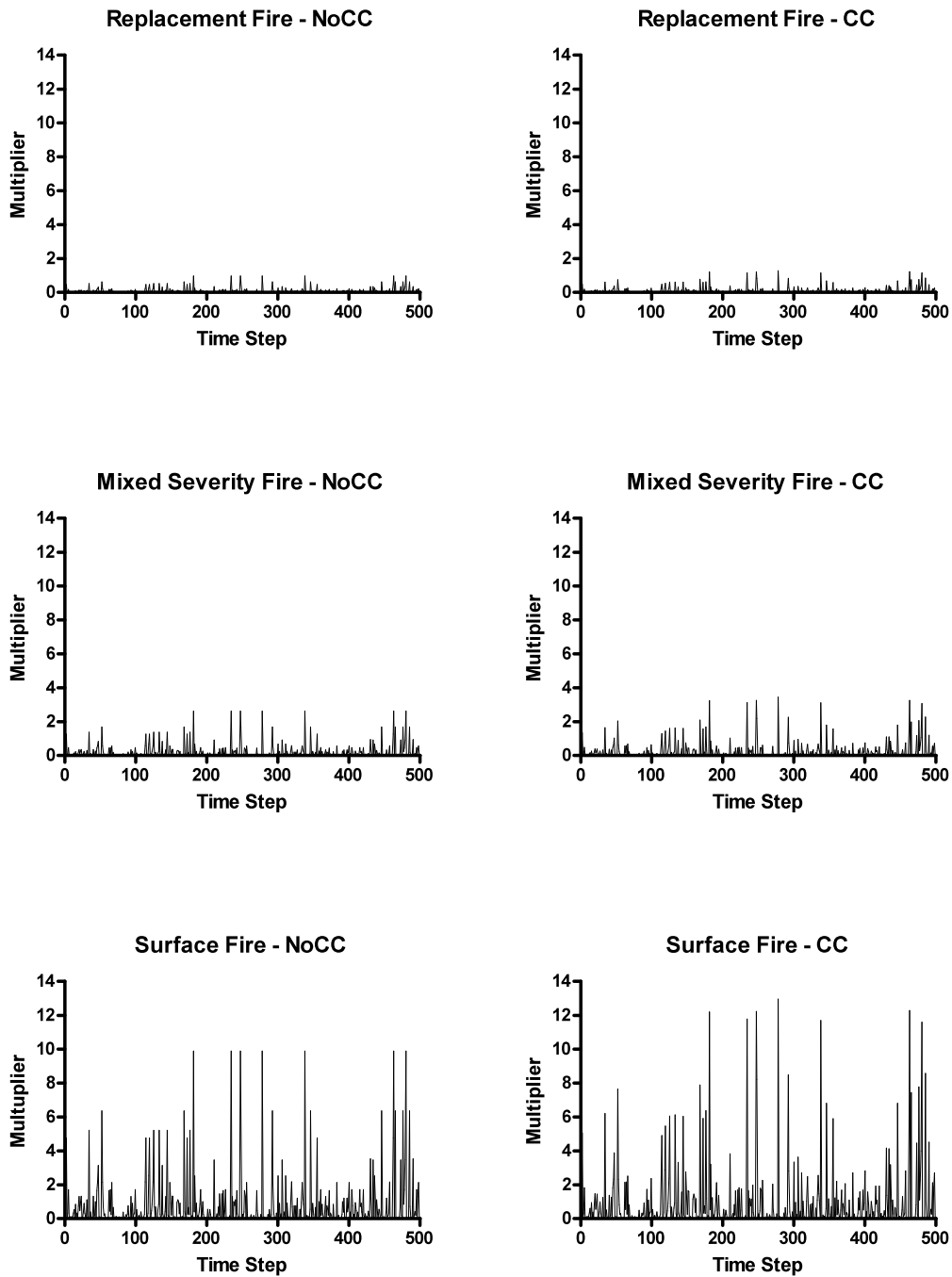
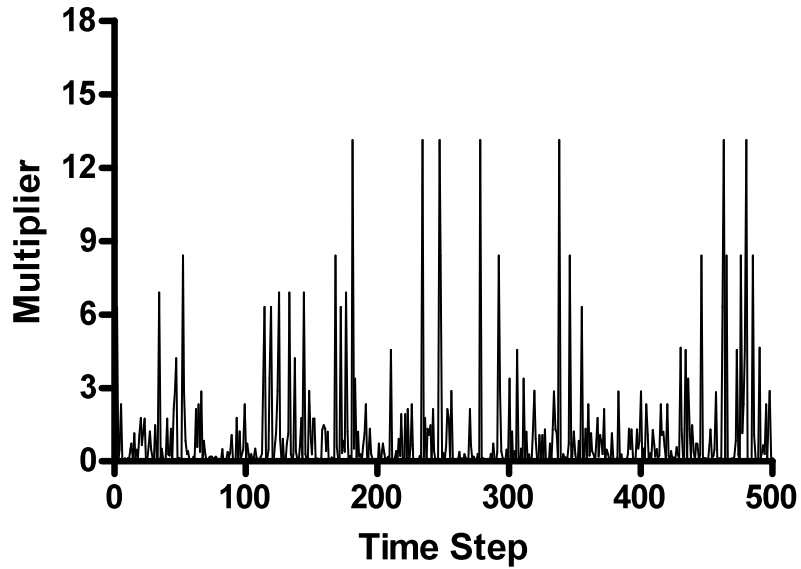


Figure A-7. Temporal multipliers of fire severity types for subalpine forest types and alpine systems on the east side of the Sierra Nevada.

East Side - Mid-Elevation Shrubland Multipliers

Replacement Fire - NoCC



Replacement Fire - CC

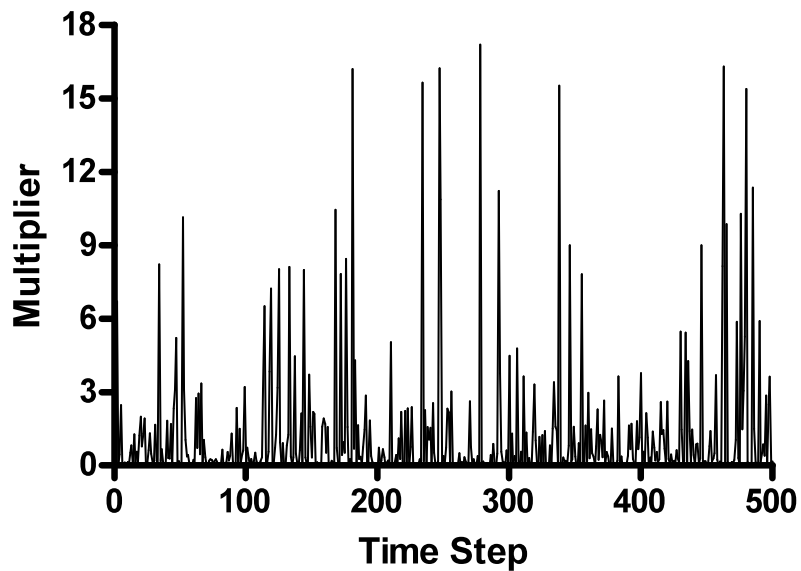
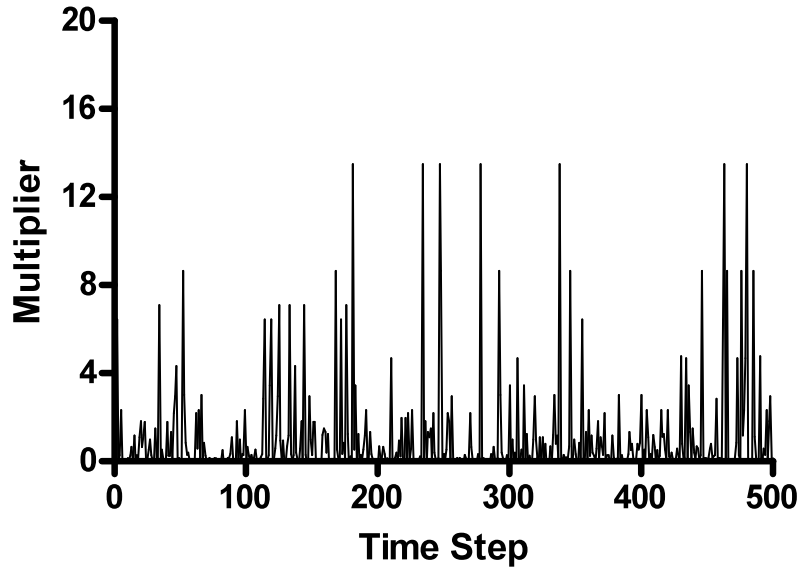


Figure A-8. Temporal multipliers of fire severity types for mid-elevation shrublands and woodlands on the east side of the Sierra Nevada.

East Side - Xeric Shrubland Multipliers

Replacement Fire - NoCC



Replacement Fire - CC

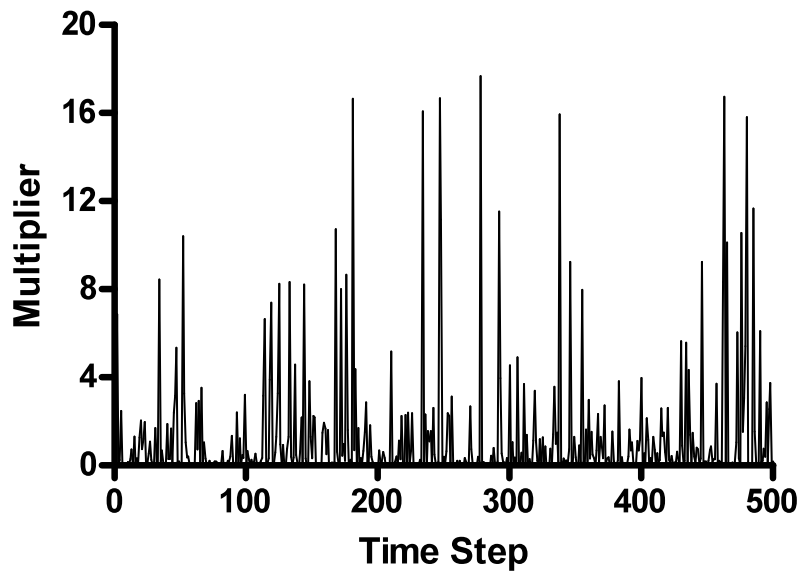


Figure A-9. Temporal multipliers of fire severity types for xeric shrublands on the east side of the Sierra Nevada.

West Side - Low Elevation Forest Fire Multipliers

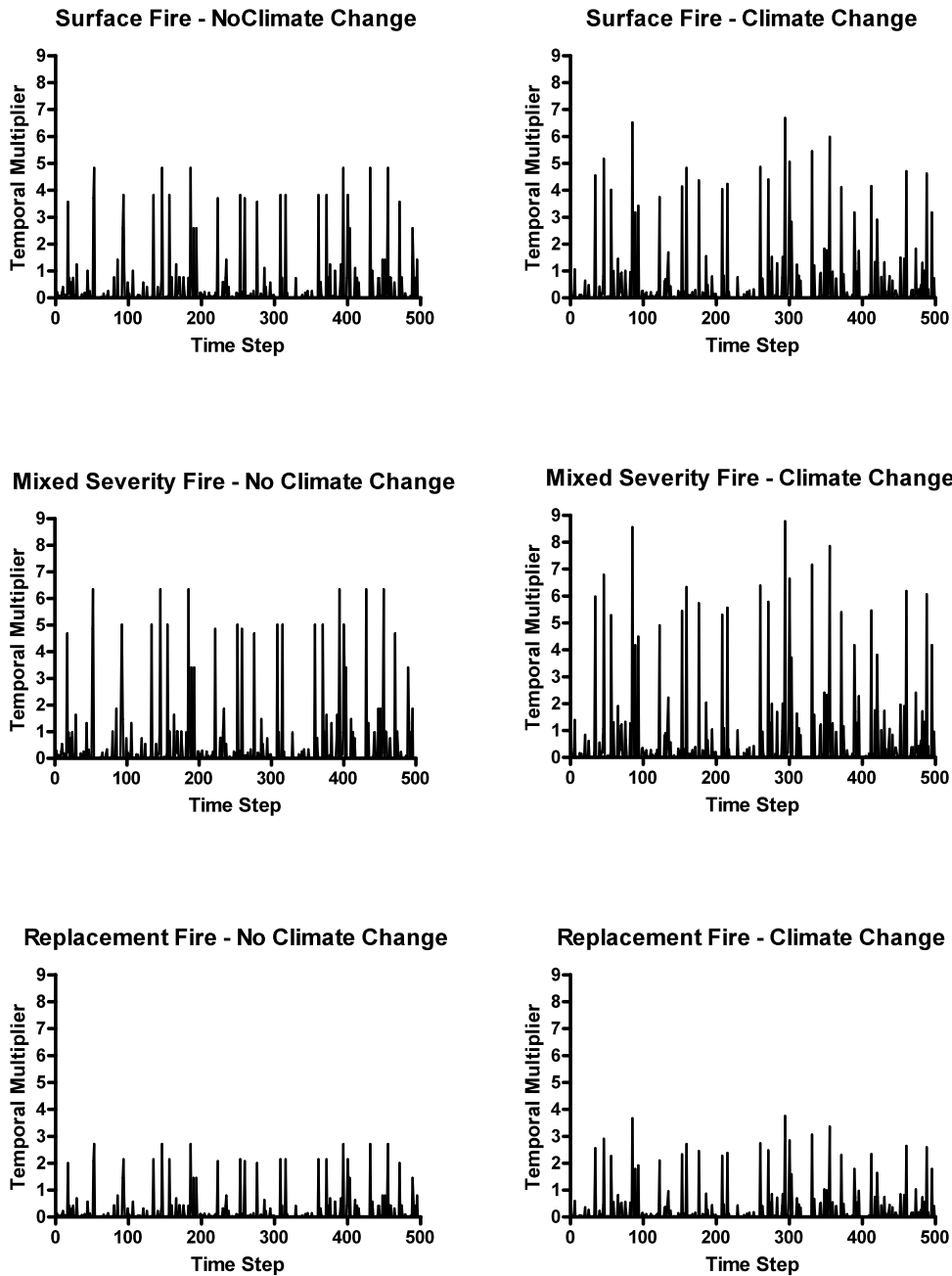


Figure A-10. Temporal multipliers of fire severity types for low-elevation forests on the west side of the Sierra Nevada.

West Side - Mid-Elevation Forest & Meadow Fire Multipliers

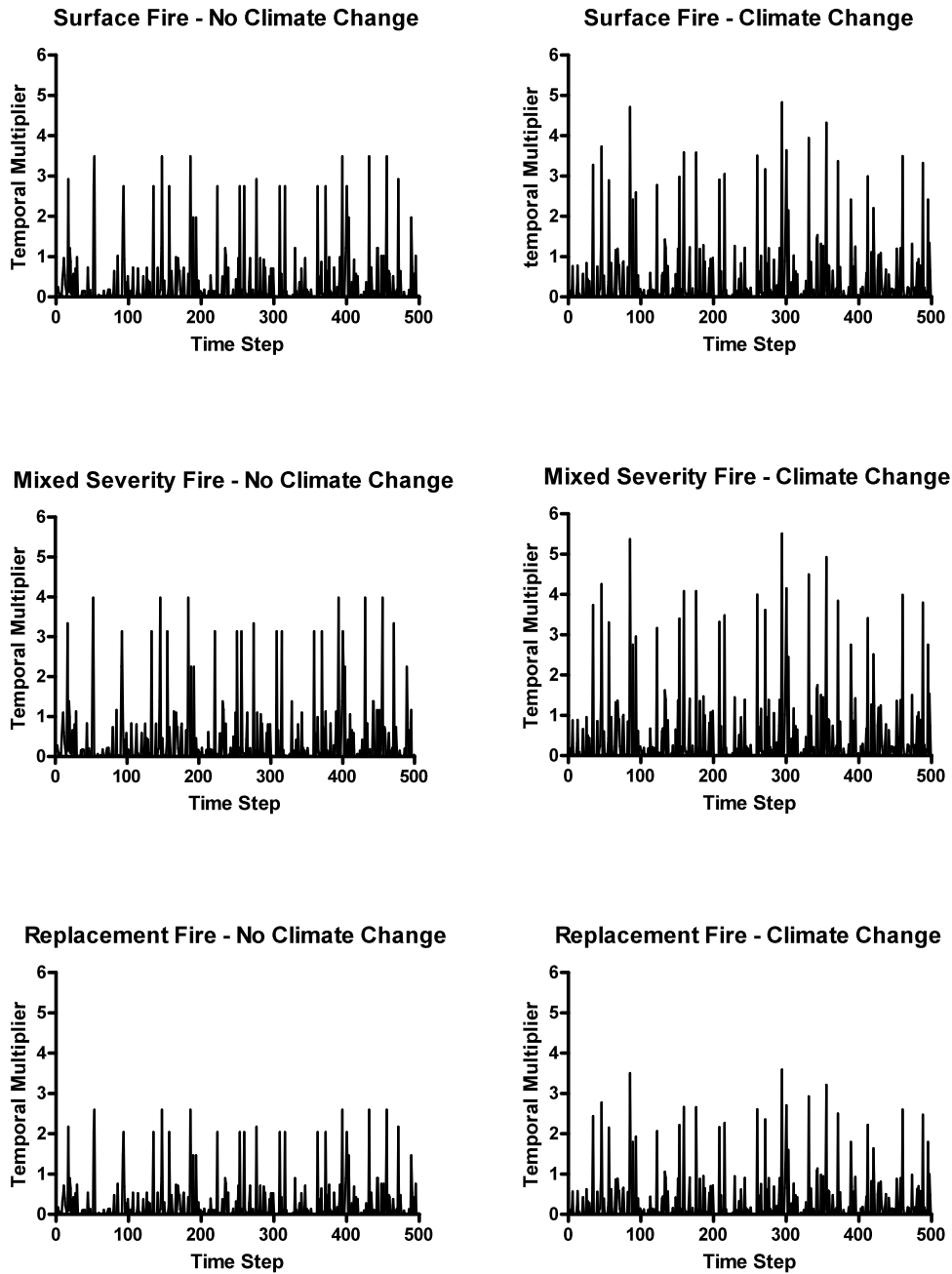


Figure A-11. Temporal multipliers of fire severity types for mid-elevation forests on the west side of the Sierra Nevada.

West Side - Subalpine Forest Fire Multipliers

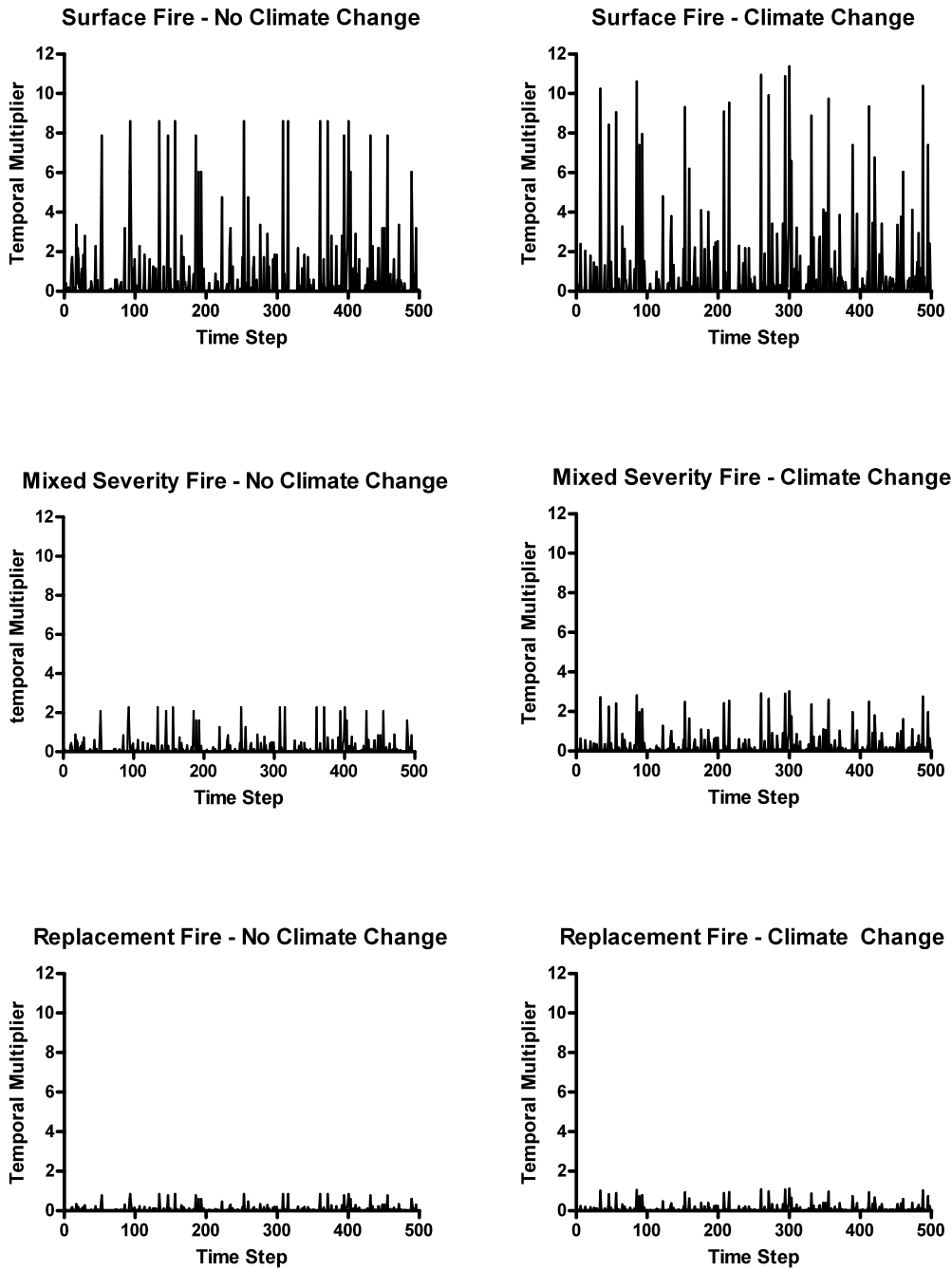
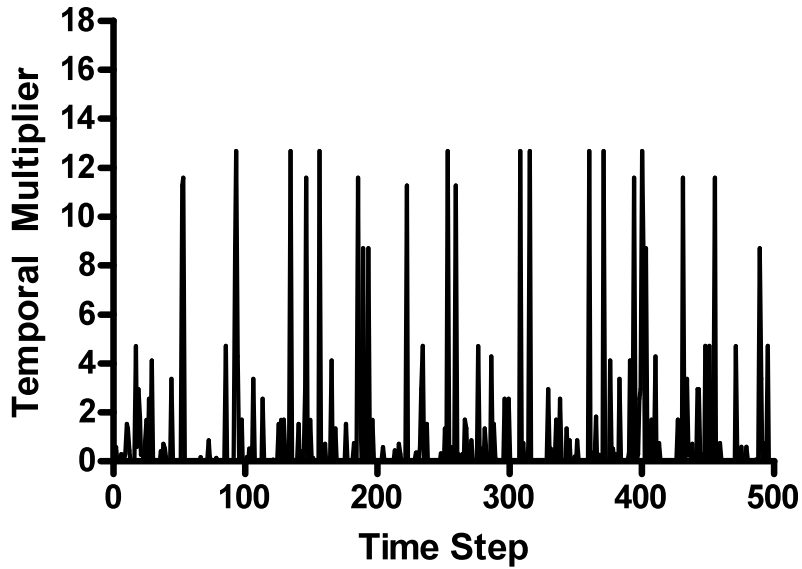


Figure A-12. Temporal multipliers of fire severity types for subalpine forests and alpine systems forests on the west side of the Sierra Nevada.

West Side - Mid-Elevation Shrubland Fire Multipliers

ReplacementFire - No Climate Change



Replacement Fire - Climate Change

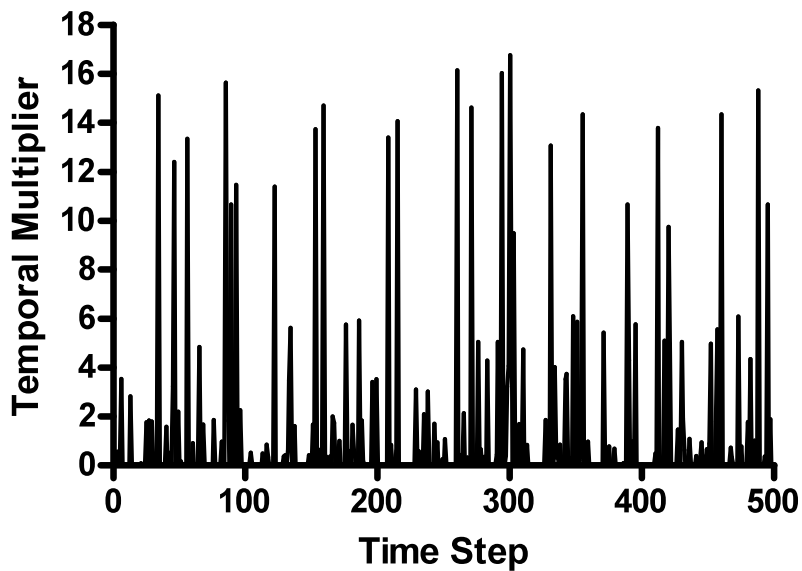
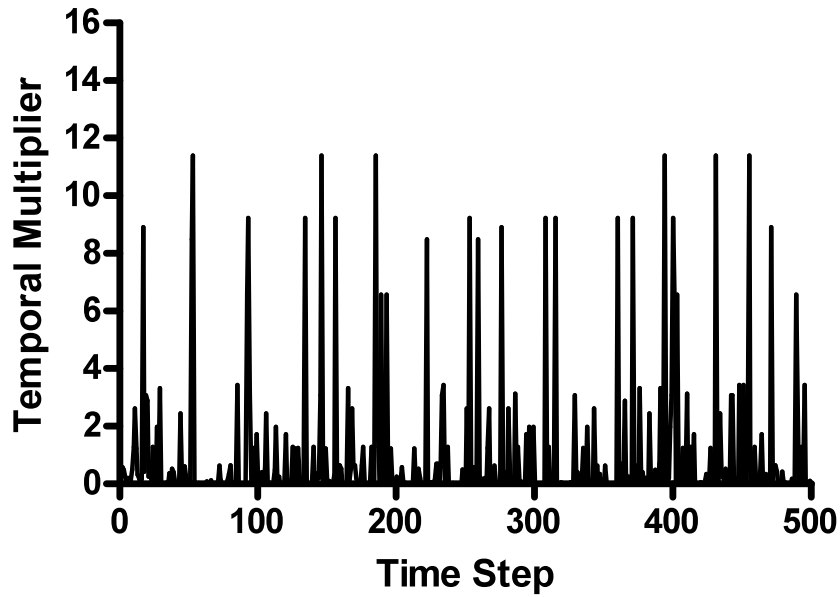


Figure A-13. Temporal multipliers of fire severity types for mid-elevation shrublands on the west side of the Sierra Nevada.

West Side - Xeric Shrubland Fire Multipliers

Replacement Fire - No Climate Change



Replacement Fire - Climate Change

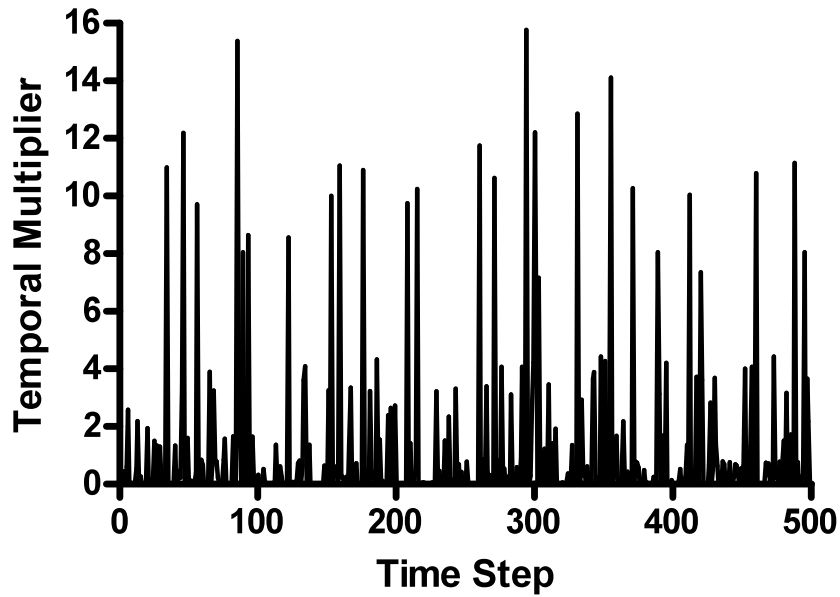


Figure A-14. Temporal multipliers of fire severity types for xeric shrublands on the west side of the Sierra Nevada.

Non-Fire Temporal Multipliers

All other temporal multipliers involved modifications to drought, invasion rates, soil moisture, and flows. Drought related temporal multipliers were the same on the east and west sides. We assumed that the new PDSI under climate change would show drier (higher temperature, less precipitation, or more evapotranspiration) conditions, which means that positive PDSI values would become smaller and that negative values would become even more negative. Although this assumption was conceptually true, the mathematical implementation of the modification is not straightforward, in part because several variables enter into the computation of PDSI (not just temperature) and its time step is monthly, not yearly (yearly PDSI is obtained through averaging) (Heddinghaus and Sabol 1991). Therefore, we arbitrarily chose to multiply yearly original PDSI values <0 (dry years) by the temperature temporal multipliers to make them more negative or drier, whereas values ≥ 0 (wet years) were divided by temporal multipliers keeping them positive but reduced (Figure A-15). This heuristic linear modification was not too unreasonable given that the real PDSI equation is also a linear formula based on past values of PDSI:

$$\text{PDSI}_t = 0.897 \times \text{PDSI}_{t-1} + \text{calibrated change in soil moisture}_t$$

where t is the month and the calibrated change in moisture can be \geq or $<$ zero (Heddinghaus and Sabol 1991).

All non-fire equations developed above (Tables A-1, A-2, and A-5) used the new PDSI for climate change simulations. One exception was the intra-specific competition equation that became:

$$= e^{-\text{TempCC} \times (\text{PDSI} + \text{abs}(\text{min}[\text{PDSI}]])} / e^{-\text{abs}(\text{min}[\text{PDSI}])},$$

where PDSI is the original time series from 1896 to 2006 and TempCC is the temperature temporal multiplier assuming climate warming. Under future drier conditions, we heuristically assumed that intra-specific competition will be more intense.

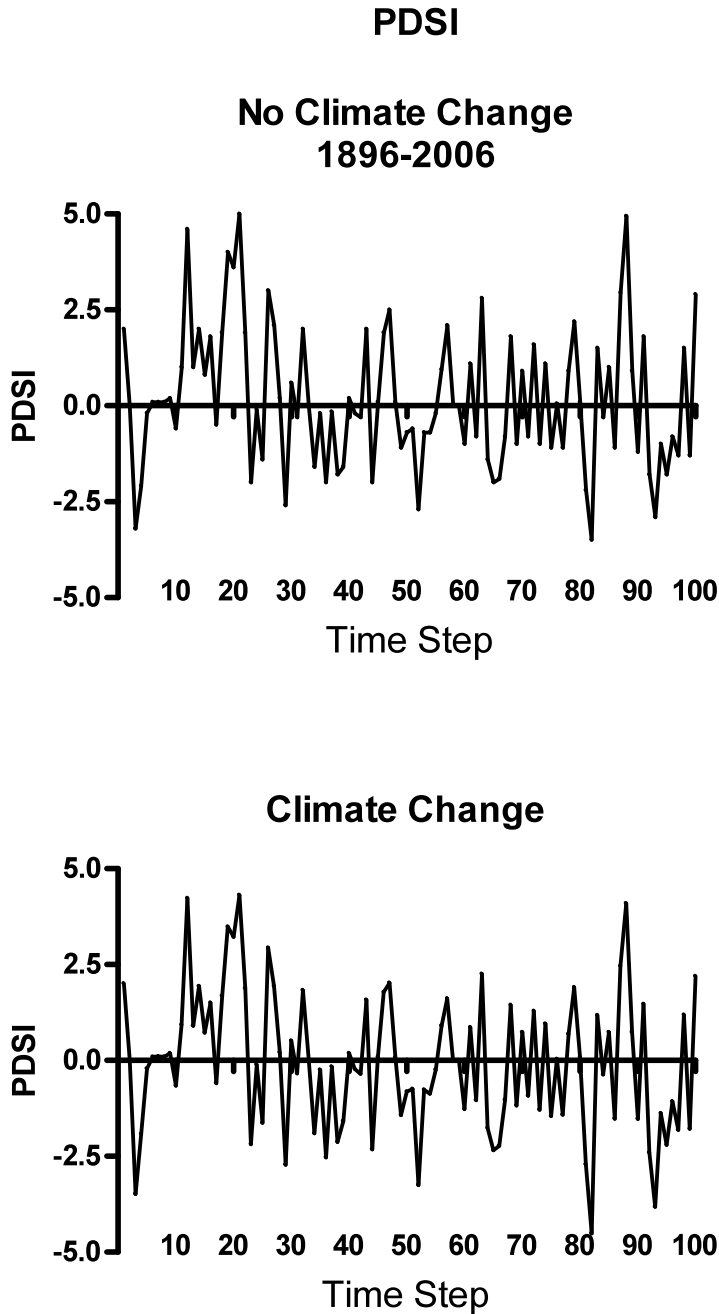


Figure A-15. PDSI for the northern Sierra Nevada from 1896 to 2006 (upper graph) and modified PDSI assuming temperatures increasing by +3°C (lower graph).

As before, flow temporal multipliers were generated with gage data from the Truckee River and Feather River. The peak flow temporal multiplier (-CC for no climate change) was modified for climate change (+CC) under the simple assumptions that peak flows and their variability increase with time due to more frequent rain-on-snow events and early snow melt.

A heuristic relationship was built in the absence of more mechanistic flow modification equation:

$$\text{Peak Flow}_{+CC} \text{ temporal multiplier} = \text{Peak Flow}_{-CC} \text{ temporal multiplier} \times (1+U \times U \times \log_{10}[\text{time-step}]),$$

where U is a random number drawn ($0 \leq U < 1$) from a uniform distribution. In this equation, peak flow increases by nearly twice over 100 years as both drawn random numbers are closer to one. The multiplication of the two independently drawn random numbers insures a highly variable time series (Figure A-16). The new time series was used to obtain 7-year, 20-year, and 100-year flood events using the same rules as described above.

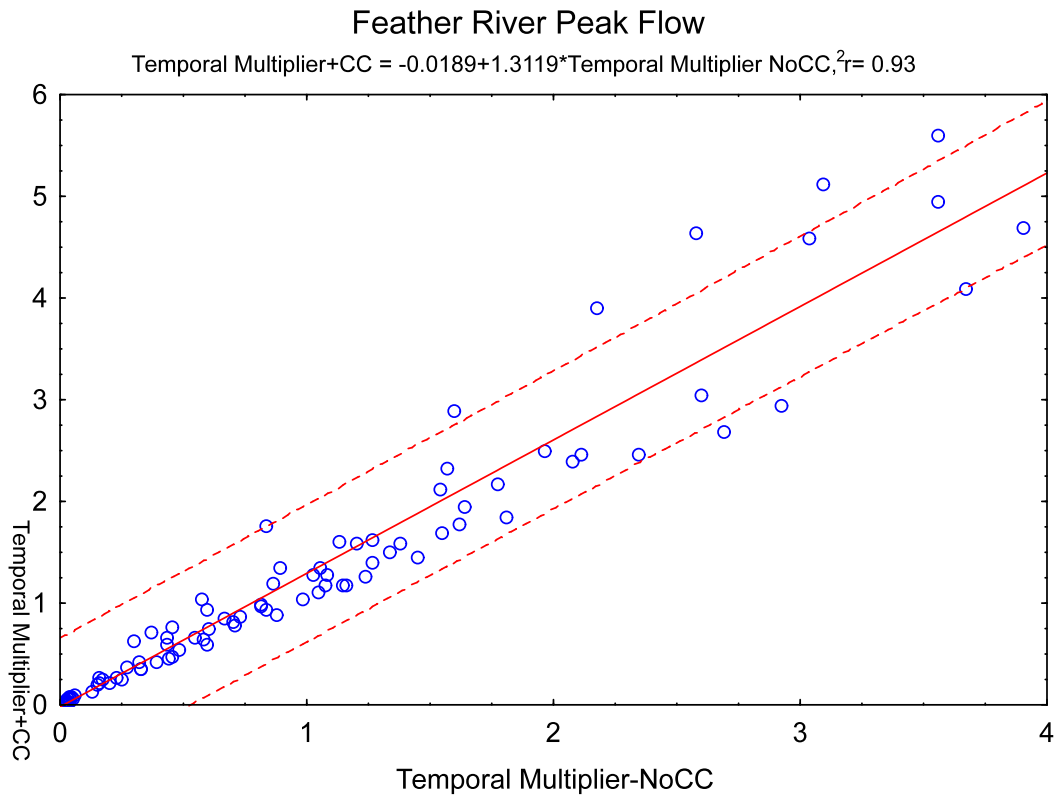


Figure A-16. Peak flow temporal multipliers without climate change versus climate change effects used to illustrate heuristic transformation using gage data from Feather River. Regression bands are $\pm 95\%$ confidence intervals. Note the slope > 1 and increasing variability with higher values.

The cottonwood and willow recruitment temporal multiplier used the new temporal multiplier for peak flow; however, the rules for successful recruitment were modified under the climate change scenario. As before, a 5% failure rate was assumed: 5% of years were randomly chosen for completely failed recruitment. For the no-climate change scenario, we had assumed that the level of peak flow during a year was the only datum that determined if enough river scouring, deposition, and wetting permitted recruitment. With climate change,

however, peak flow was predicted to occur increasingly earlier (Maurer 2007) and before flowering and seed deposition of cottonwood and willow. (We also assumed that cottonwood and willow flowering would not “catch up” with earlier flows because of potential genetic constraints and persistent cold air drafting in drainages.) Therefore, recruitment was increasingly uncertain with time due to the mismatch of peak flow and flowering. Maurer’s (2007) estimates of uncertainty (of earlier flow occurring) for periods of 30 years under the “business-as-usual” scenario of the PCM model were used to reduce recruitment success: 87% for years 1 to 30; 74% for years 31 to 60; and 61% for years 61 to 100. To determine successful recruitment the product of this uncertainty (as a proportion) and the peak flow temporal multiplier with climate change needed to be >0.77 (as before without climate change); otherwise the resulting temporal multiplier was zero. In summary, the onset of future peak flow will always have a depressing effect on cottonwood and willow recruitment, but future peak flow can be higher and more variable and compensate for loss of recruitment success.

The *low-flow-kill* temporal multiplier shared a similar heuristic equation as that of peak flow, with the exception that the temporal multiplier was the inverse of the average August and September flow (= low flow) multiplied by the correction factor for climate change:

*Low-flow-kill*_{+CC} temporal multiplier

= $1 / \{ \text{low flows}_{-CC} \text{ temporal multiplier} \times (1 + U \times U \times \log_{10}[\text{time-step}]) \} > 1$;

= 0 if $1 / \{ \text{low flows}_{-CC} \text{ temporal multiplier} \times (1 + U \times U \times \log_{10}[\text{time-step}]) \} \leq 1$.

We hypothesized that carbon from enhanced atmospheric green house gases would fertilize exotic forb species growth, seed or root production, and invasion of uninfested areas if the floodplain was sufficiently wetted by annual (not peak) flows (Bradley 2009; Smith et al., 2000). The temporal multiplier for exotic forb invasion was simply the year by year multiplication of the green house gases temporal multiplier and the annual flow temporal multiplier (i.e., more infestation during years of higher annual flows and more atmospheric carbon), divided by 0.6, which is about the annual flow realized on the Truckee during a year with a 5-year flow (Figure A-17). This correction factor insured that only the lowest annual flow depressed exotic forb invasion.

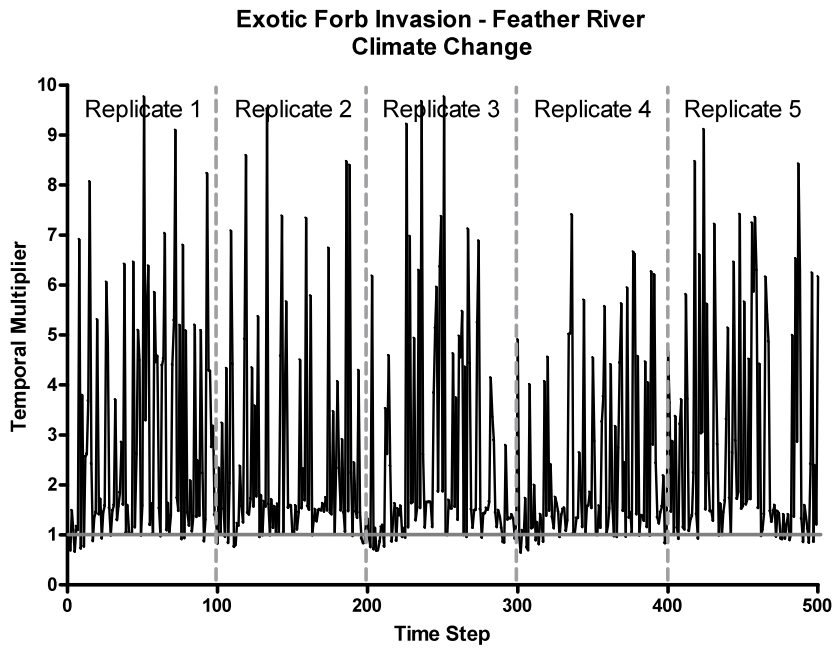
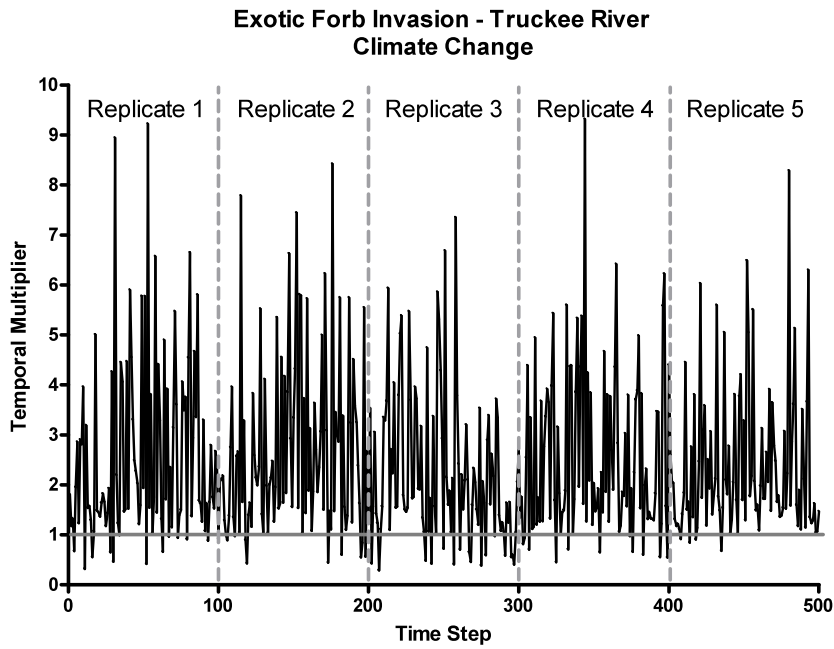


Figure A-17. Temporal multipliers for exotic forb invasion under a climate change scenario of increasing green house gases.

Using VDDT to Simulate Vegetation Conversions

To simulate potential future shifts in biophysical settings, we first determined the *rate* of projected shift, and then determined the *type* of projected vegetation shift.

As described in Section 3, we used future “climate envelope” projections for major tree and shrub species to show predicted *rates* of stress over the next 80 years for the associated biophysical settings. The rate of stress in the VDDT models was the proportion of a biophysical setting experiencing stress as calculated in Section 3 divided by the number of years projected (i.e., 80 years). Projected stress areas for a given species were assumed to equate with likely conversion because the species would not reproduce under the new climatic conditions. It was realized that a biophysical setting might persist beyond the 80 years of predicted stress because adult trees can survive although their offspring fail to establish. To minimize this problem, biophysical setting conversion in the models only occurred when a stand replacing disturbance killed adults; in other words, a biophysical setting could persist for longer than predicted if it did not experience significant stand replacing events, even assuming increased disturbance rates with climate change. This adjustment led to another problem: some subalpine and aspen biophysical settings that were predicted to experience very high levels of stress did not experience vegetation shifts rapid enough to “keep up” with predicted stress over 80 years because the natural disturbance rates are too slow (for example, a long mean fire return interval). In these cases, 100% of all stand replacing events caused a vegetation shift, although conversion was still not “fast enough.”

To forecast the *type* of biophysical settings that would replace a stressed one, we used Dr. Jim Thorne’s data on actual vegetation conversions based on the analysis of Wieslander Vegetation Type data for the Sierra Nevada. The critical assumption made here was that vegetation transitions from the last 80 years were the best guess to future transitions for our VDDT simulations with climate change effects. Moreover, no other data were available. The conversion first required a crosswalk between the California Wildlife Habitat Relationship classification (WHR) used by Thorne et al. (2008) and biophysical settings (Table A-6).

Table A-6. Biophysical settings and California Wildlife Habitat Relationship classification (WHR) crosswalk.

Functional Group	Biophysical Setting	WHR
Alpine & Subalpine		
	Subalpine meadow	WTM
	Alpine Shrubland	ADS
	Lodgepole Pine-dry	LPN
	Lodgepole Pine-wet	LPN
	Subalpine Woodland	SCN
	Red Fir-Western White Pine	RFR
	Red Fir-White Fir	RFR
Mid-Elevation Forest		

	Mixed Conifer-Mesic	WFR, SMC, DFR
	Yellow Pine East Side	EPN, JPN
	Ponderosa Pine-Mixed Conifer	PPN
	California Oak-Pine Forest	MHC, MHW
	Wet Meadow	WTM
	California Montane Riparian	MRI
	Great Basin Montane Riparian	MRI
Mid-Elevation Eastern Shrubland		
	Montane sagebrush Steppe	SGB, BBR
	Big Sagebrush Shrubland	SGB, BBR
	Low Sagebrush	LSG
	Pinyon-Juniper Woodland	PJN
	Curlleaf Mountain Mahogany	PJN
	Aspen Woodland	ASP
	Aspen-Mixed Conifer Forest	ASP
Xeric-Shrubland		
	Ultramafic Woodland and Chaparral	MCH, MCP
	Montane Chaparral	MCH, MCP
Lower-Elevation-Western Forest & Woodland		
	California Mixed Evergreen Forest	MHC, MHW
	Blue Oak-Pine Foothill Woodland	BOP, BOW

Thorne's matrix of type conversions allowed us to convert VDDT virtual pixels from an original type to new types over time (~80 years) as dictated by the recalculated proportions (i.e., after elimination of "false" conversions) in the conversion matrix. (See main text Section 5 for the distinction between true and false vegetation shifts.)

The data for true conversion when more than one transition pathways were documented were used to split proportionally the rate of transition (previous paragraph) using proportions calculated from the Thorne data. Several steps were involved in the calculations of vegetation shifts:

1. Calculate the total rate of replacement events: Obtain the realized rate (probability/year) of each replacement disturbance from the *non-climate change* simulation (assuming *minimum management*) for the out-going biophysical setting. The rates of different disturbance types (for example, replacement fire and mixed severity fire) are summed according to their contributions to the early succession class. For example, replacement fire had a rate 0.0026/yr and mixed severity fire of 0.0148/yr in ponderosa pine; however mixed severity fire contributed only 25% to the

early succession class, whereas replacement fire fully contributed to this class. Therefore, the weighted sum of replacement events = $0.25 \times 0.0148 + 1 \times 0.0026 = 0.0063$.

2. Calculate total loss of “virtual pixels” from originating biophysical setting: During the 80-year period of simulation, a certain proportion of a biophysical setting’s area per year flows away from the out-going vegetation. This value is determined by the division of the percentage of the area of the biophysical setting stressed (as calculated in Section 3 of main text) by the total rate of replacement events. To continue the example, approximately 6.6% of the ponderosa pine biophysical setting of today will be stressed during the next 80 years; as a result the realized loss of this biophysical setting will be 0.131 or 0.066 divided by 80 years and divided by 0.0063, which is the magnitude of realized replacement events.
3. Split the loss to recipient biophysical setting(s) (i.e., vegetation shift): The loss per year of area (or virtual pixels) was allocated according to Thorne’s recalculated proportions to in-coming biophysical settings (i.e., biophysical settings that received pixels from out-going biophysical setting). To complete the example, approximately 85.3% of stressed ponderosa pine being lost at the above rate of 0.131 will convert to California mixed evergreen and 14.7% to chaparral.
4. Split the disturbance rates in the losing biophysical setting: To simulate this calculated outcome, split all replacement disturbances in the original biophysical setting model. In the ponderosa pine example, the original replacement rates are split in three proportions for each of replacement fire and mixed fire:
 - a. No conversion = $1 - 0.131 = 0.869$ for replacement fire
 - b. Conversion to California mixed evergreen = $85.3\% \times 0.131 = 0.112$ for replacement fire
 - c. Conversion to chaparral = $14.7\% \times 0.131 = 0.019$ for replacement fire
 - d. The three rates above are each multiplied by 0.25 to obtain the conversion proportion based on the contribution of mixed severity fire, which was 25% top-kill.
5. These proportions are implemented in every model’s appropriate pathways.

Simulations will generate new pixels for in-coming biophysical settings in the model of the out-going one. In the final accounting of area for ecological departure calculation, the new pixels must be added to the results of another independent model representing the recipient biophysical setting. Ideally, all inter-connected models should be simulated in a single “Uber” model, which is the more recent modeling approach we use.

References

- Barrett, T.M. 2001. Models of vegetation change for landscape planning: a comparison of FETM, LANDSUM, SIMPLLE, and VDDT. USDA Forest Service General Technical Report RMRS-GTR-76-WWW.
- Beukema, S.J., W.A. Kurz, C.B. Pinkham, K. Milosheva, and L. Frid. 2003. Vegetation Dynamics Development Tool, User's Guide, Version 4.4c. Prepared by ESSA Technologies Ltd.. Vancouver, BC, Canada, 239 p.
- Bestelmeyer, B.T., Brown, J.R., Trujillo, D.A., Havstad, K.M., 2004. Land management in the American Southwest: a state-and-transition approach to ecosystem complexity. *Environmental Management* 34: 38-51.
- Bradley, B.A. 2009. Regional analysis of the impacts of climate change on cheatgrass invasion shows potential risk and opportunity. *Global Change Biology* 15: 196-208
- Dettinger, M.D., D.R. Cayan, M.K. Meyer, and A.E. Jeton. 2004. Simulated hydrologic responses to climate variations and change in the Merced, Carson, American River basins, Sierra Nevada, California, 1900-2099. *Climatic Change* 62: 283-317.
- Hann, W.J., Bunnell, D.L., 2001. Fire and land management planning and implementation across multiple scales. *International Journal of Wildland Fire* 10: 389-403.
- Heddinghaus, T.B., Sahol, P. 1991. A Review of the Palmer Drought Severity Index and Where Do We Go From Here? Proc. 7th Conf. on Applied Climatology, Salt Lake City, Utah. p. 242-246.
- Intergovernmental Panel on Climate Change. 2007. *Climate Change 2007: Impacts, Adaptation and Vulnerability. Contribution of Working Group 1 to the Fourth Assessment Report of the IPCC.* Cambridge University press, Cambridge, UK.
- Low, G., Provencher, L., Abele, S.A., 2010. Enhanced conservation action planning: assessing landscape condition and predicting benefits of conservation strategies. *Journal of Conservation Planning* 6:36-60.
- Maurer, E.P. 2007. Uncertainty in hydrologic impacts of climate change in the Sierra Nevada, California, under two emissions scenarios. *Climatic Change* 82: 309-325.
- McBride, J.R., Strahan, J. 1984. Establishment and survival of woody riparian species on gravel bars of an intermittent stream. *American Midland Naturalist* 112:235-245.
- Provencher, L., Campbell, J., Nachlinger, J., 2008. Implementation of mid-scale fire regime condition class mapping. *International Journal of Wildland Fire* 17: 390-406.
- Provencher L., G. Low G., Abele S., 2009. Bodie Hills Conservation Action Planning. Final Report to the Bureau of Land Management Bishop Field Office, The Nature Conservancy, <http://conserveonline.org/library/>
- Rollins, M.G. 2009. LANDFIRE: a nationally consistent vegetation, wildland fire, and fuel assessment. *International Journal of Wildland Fire* 18:235-249.
- Rood, S.B., C.R. Gourley, E.M. Ammon, L.G. Heki, J.R. Klotz, M.L Morrison, D. Mosley, G.G. Scoppettone, S. Swanson, and P.L. Wagner. 2003. Flows for floodplain forests: A successful riparian restoration. *BioScience* 53: 647-656.

- Shlisky A.J., Hann W.J., 2003. Rapid scientific assessment of mid-scale fire regime conditions in the western US. In 'Proceedings of 3rd International Wildland Fire Conference', 4–6 October. Sydney, Australia.
- Smith, S.D., T.E. Huxman, S.F. Zitzer, T. N. Charlet, D.C. Housman, J.S. Coleman, L.K. Fenstermaker, J.R. Seemann, and R.S. Nowak. 2000. Elevated CO₂ increases productivity and invasives species success in an arid ecosystem. *Nature* 408:79-82.
- Taylor, A.H., Beaty R.M., 2005. Climatic influences on fire regimes in the northern Sierra Nevada mountains, Lake Tahoe Basin, Nevada, USA. *Journal of Biogeography* 32: 425–438
- Thorne, J.H., Morgan, B.J., and Kennedy, J.A. 2008. Vegetation change over sixty years in the central Sierra Nevada, California, USA, *Madrono* 55:223-237.
- Westerling, A. L.: "Climate Change Impacts on Wildfire," Chapter 12 in *Climate Change Science and Policy*, Schneider, Mastrandrea, and Rosencranz, Eds., Island Press. *in press*, (English edition)
- Westerling, A.L. and B.P. Bryant, 2008: "Climate Change and Wildfire in California," *Climatic Change* 87: s231-249. DOI:10.1007/s10584-007-9363-z.
- Westerling, A.L., Hidalgo H.G., Cayan D.R., Swetnam T.W., 2006. Warming and Earlier Spring Increase Western U.S. Forest Wildfire Activity. *Science* 313: 940 - 943.

Appendix B

Historical climate and projected future climate changes

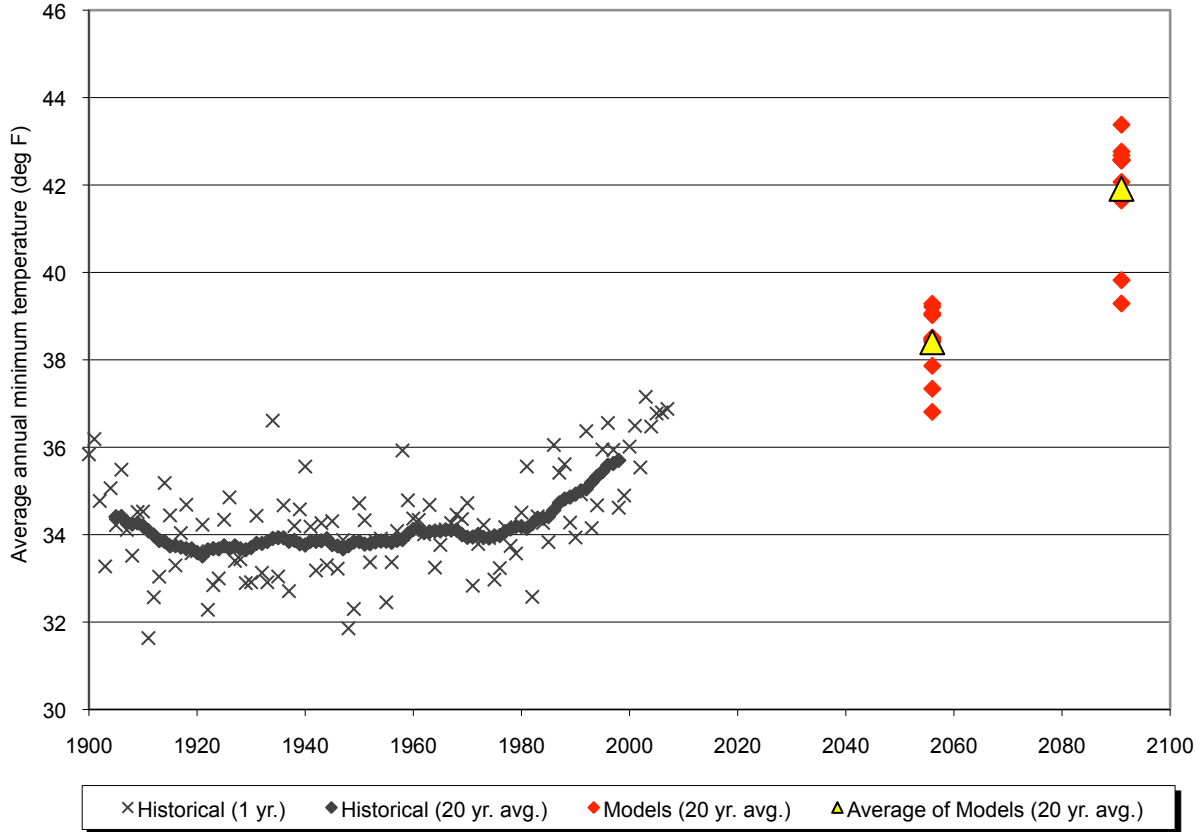


Figure B1: Historical and projected future average annual minimum temperatures for the Northern Sierra Partnership (NSP) region.

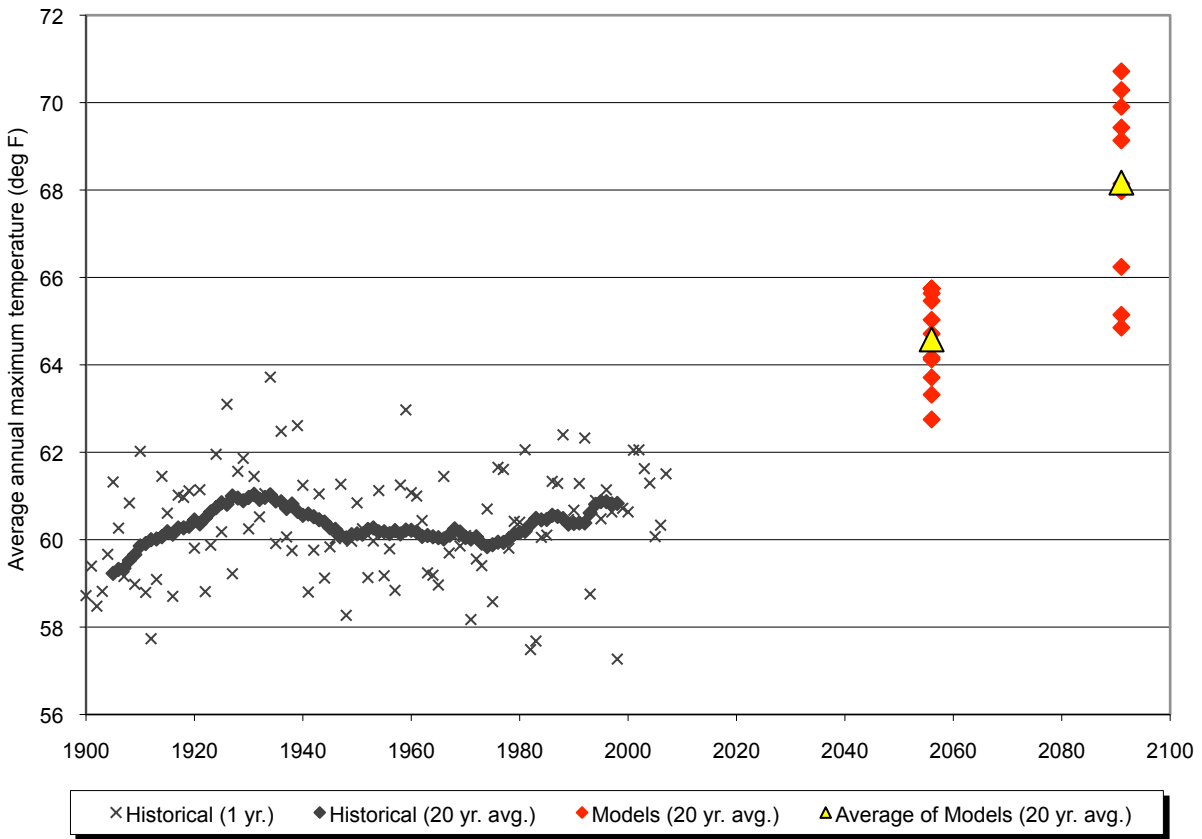


Figure B2: Historical and projected future average annual maximum temperatures for the Northern Sierra Partnership (NSP) region.

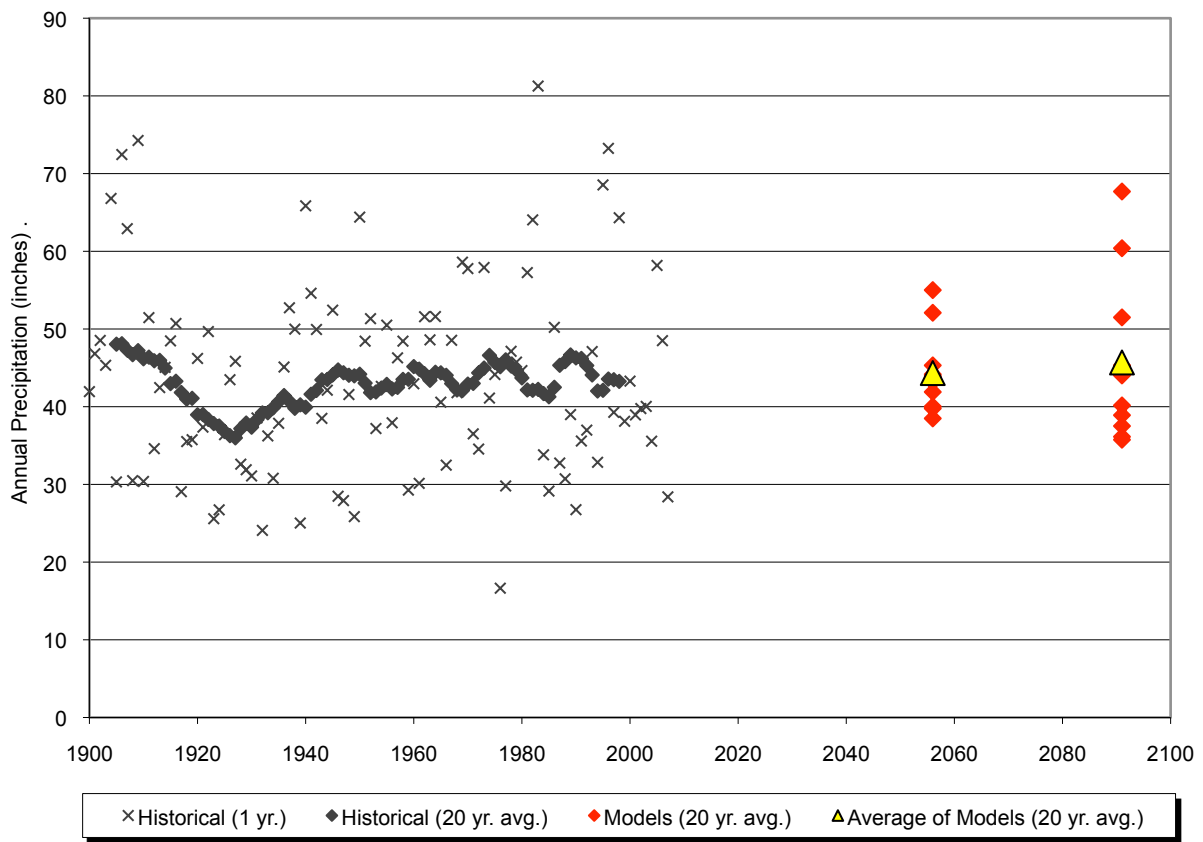


Figure B3: Historical and projected future annual precipitation for the Northern Sierra Partnership (NSP) region.

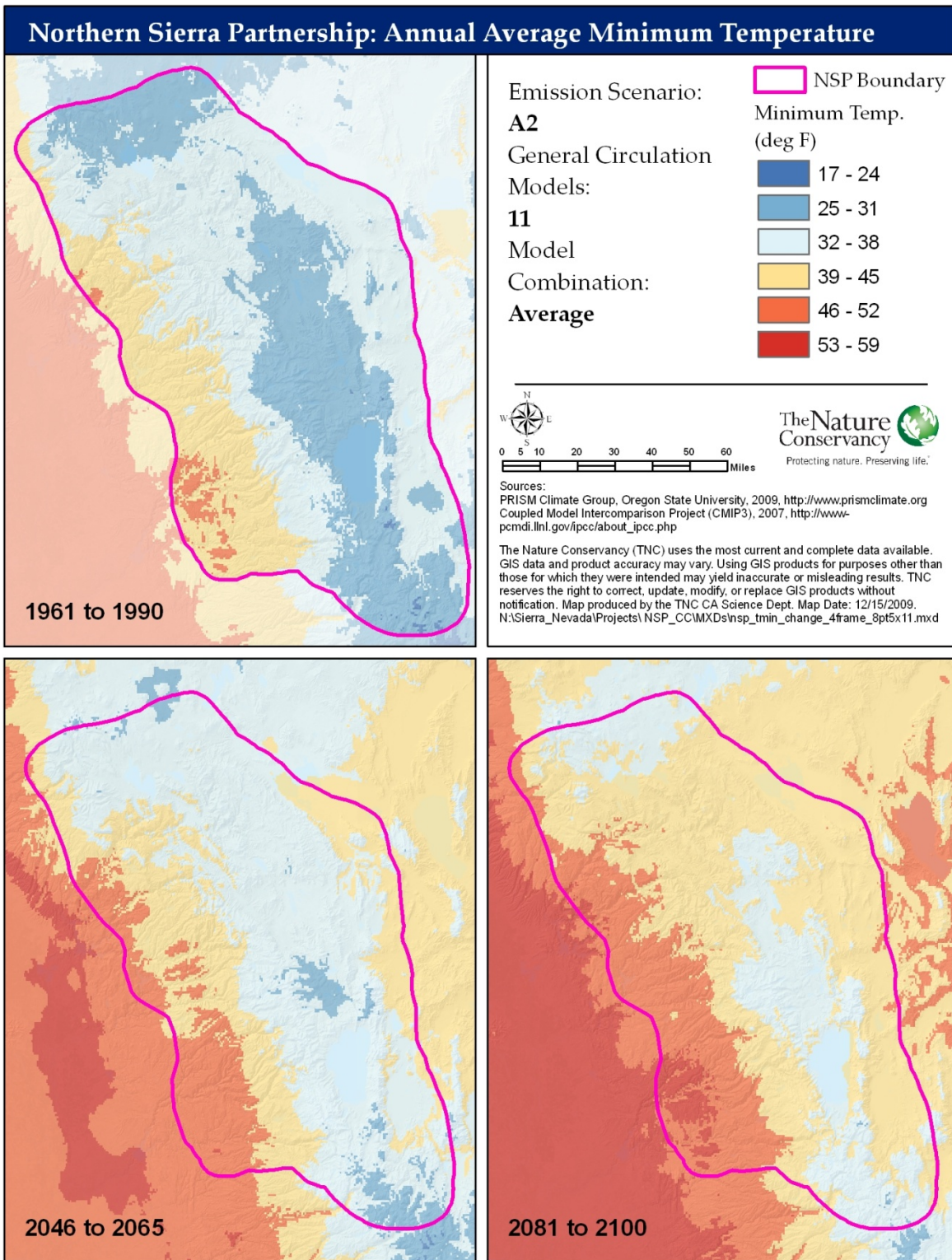


Figure B4: Maps of average annual minimum temperature change across the NSP region

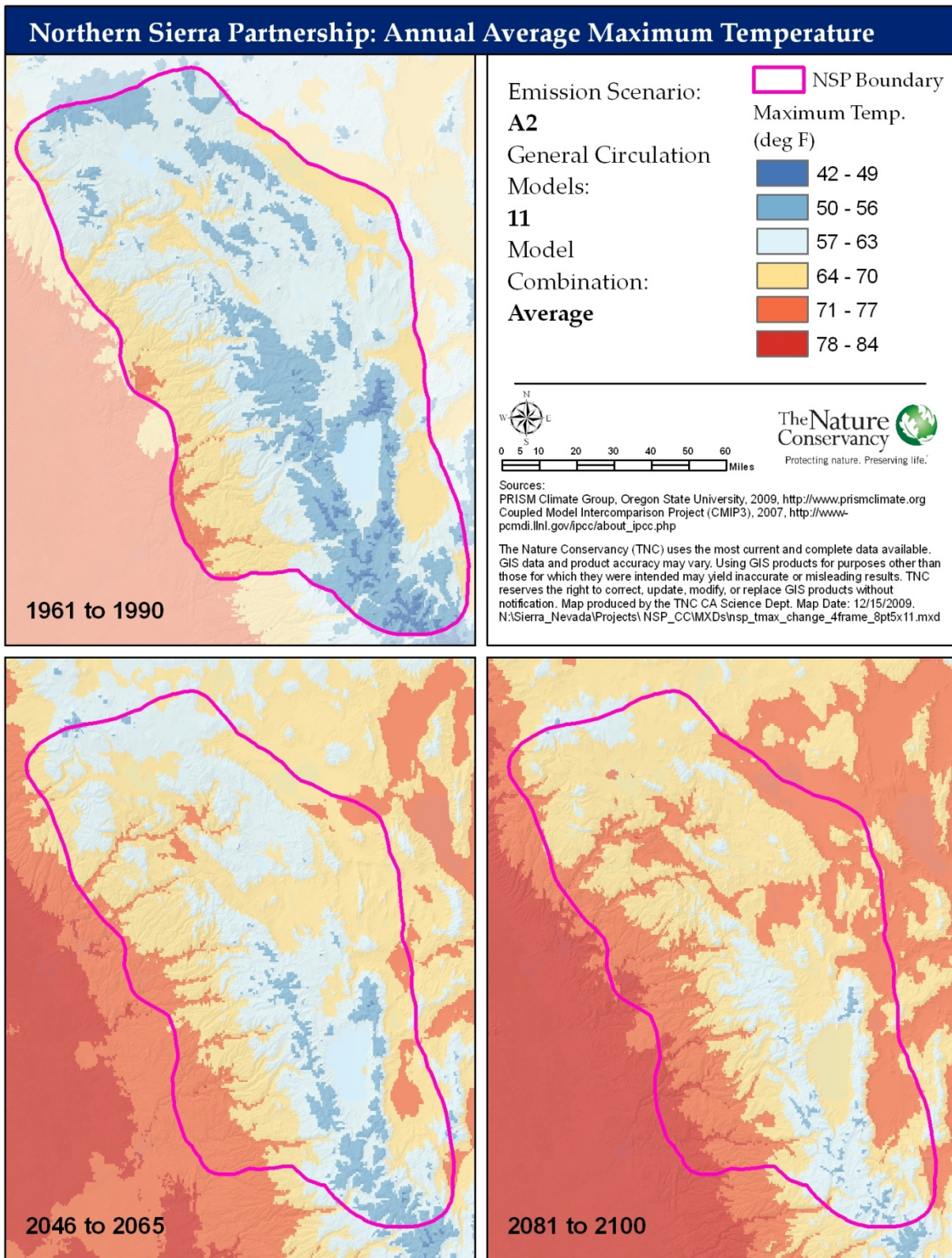


Figure B5: Maps of average annual maximum temperature change across the NSP region

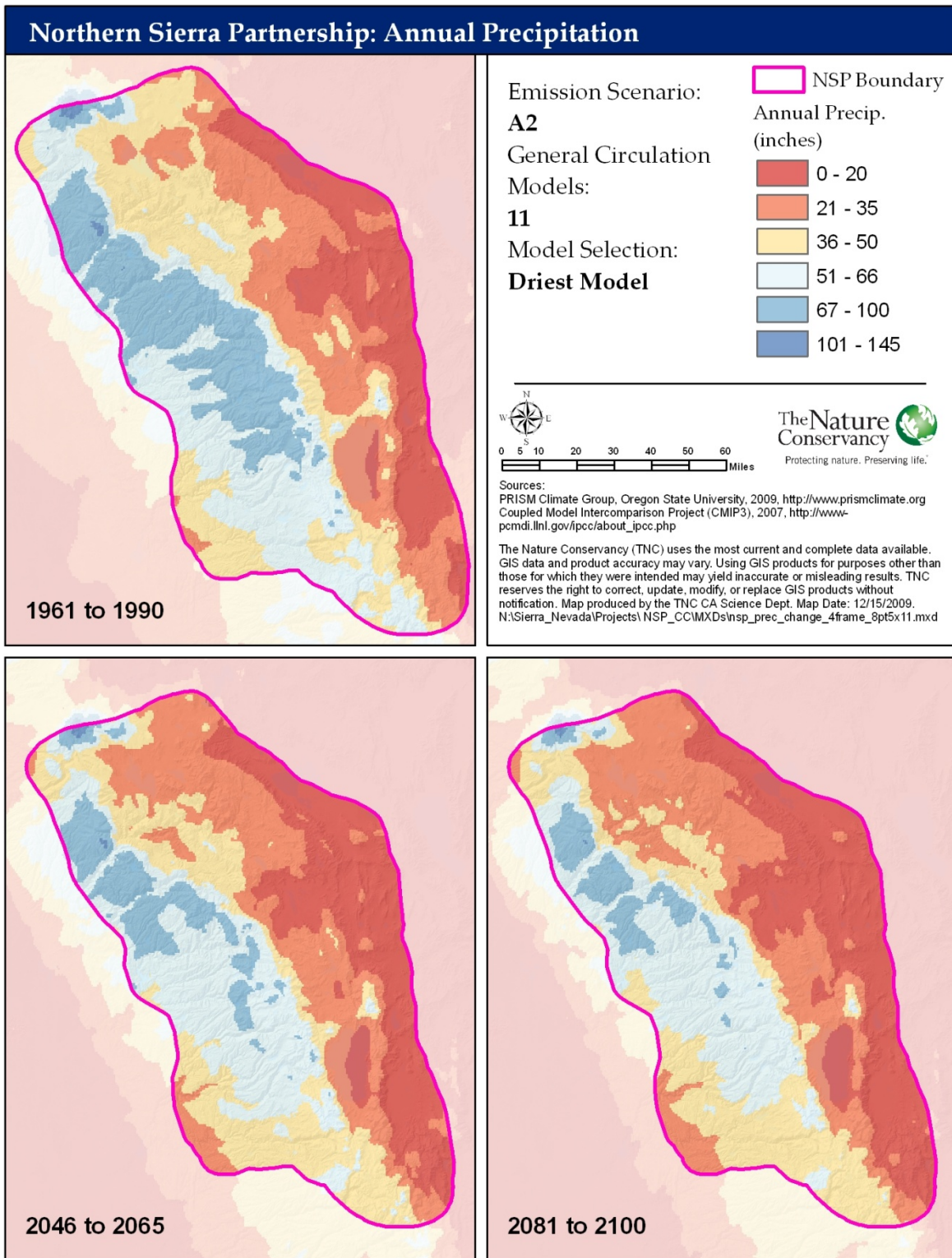


Figure B6: Maps of annual precipitation change as forecast by the driest model across the NSP region

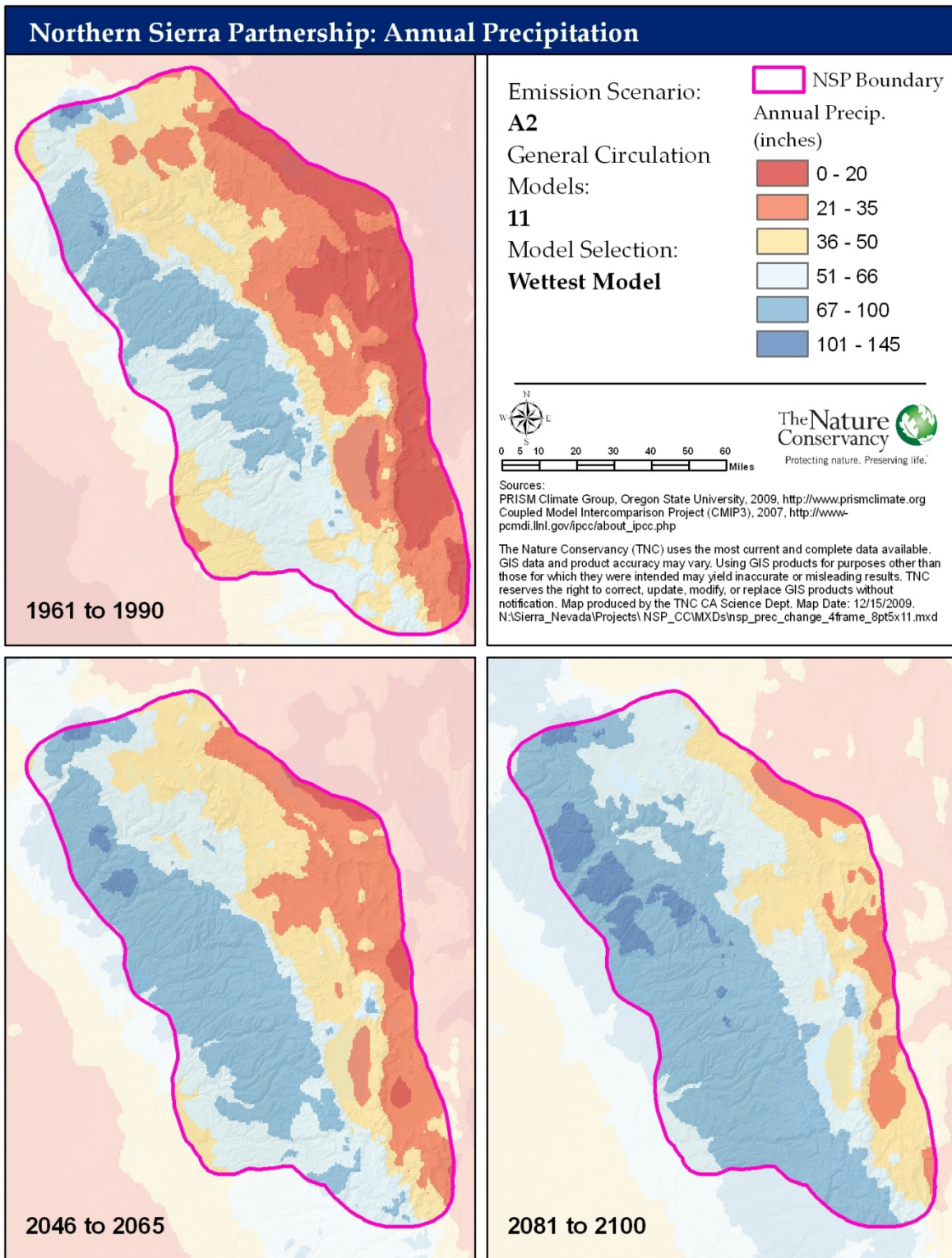


Figure B7: Maps of annual precipitation change as forecast by the wettest model across the NSP region

Appendix C

Descriptive Summary of Ecological Departure for 25 Northern Sierra Ecological Systems

Summary

Ecological departure measures an ecological system's departure from its natural range of variability (NRV). It is an integrated, landscape-scale metric that takes into account species composition, seral structure, and all relevant disturbances. Scores are graded on a scale of 0 to 100. The higher the score, the more the ecosystem is "out of whack."

Ecological departure was assessed using LANDFIRE satellite imagery, supplemented by other data, for 25 Northern Sierra ecological systems over an area of approximately 5,000,000 acres. Northern Sierra ecological systems range from good to poor current condition. All occurrences under 500 acres were not scored, size per LANDFIRE recommendations.

- Ten ecological systems are currently in good condition (i.e., low departure), including the region's largest forest system and the three smallest systems:
 - Alpine shrubland
 - Aspen woodland
 - California mixed evergreen
 - Low sagebrush
 - Mixed conifer-mesic
 - Montane chaparral
 - Montane sagebrush steppe
 - Pinyon-juniper woodlands
 - Subalpine meadow
 - Subalpine woodland
- Three ecological systems are in poor condition (i.e., high departure). Two of these are attributable to uncharacteristic native species -- Great Basin riparian (uncharacteristic native species) and wet meadows (conversion to pastureland).
- Twelve (12) other ecological systems are moderately departed from NRV, including four other large-scale conifer forest systems. The current departure for most of these ecosystems can likely be largely attributed to fire suppression or invasive species.

Ecological System Assessment

In general, the overall Eastside & Westside departure scores are more accurate than scores that were calculated for the 10 individual watersheds, due to larger sample sizes. Conditions for individual watersheds will be noted only when there is a substantial variance from the mean and sufficient acres in the occurrence.

- Alpine Shrubland rates as good condition. It is a simple system with only two vegetation classes, with almost all found in the dominant class with low-growing perennials. It is the second-smallest ecosystem in the region (1,600 acres).

- Aspen-Mixed Conifer Forests are generally lacking early succession vegetation and have too much conifer-dominated late succession. They are in better shape in the Truckee River and Middle Fork Feather River watersheds than elsewhere.
- Aspen Woodland is found almost exclusively on the eastside, and is generally in good condition. However, it also has too much senescing clones in the late succession class that are opening up and a shortage of early succession vegetation.
- Big Sagebrush Shrubland is found 99% on the eastside, where it is in fair condition due to virtually no early succession classes as well as the presence of invasive species. (It shows as good condition on the westside, but with only a small acreage in the North Fork Feather River watershed.)
- Blue Oak-Pine Foothill Woodland is found exclusively on the Westside (with only 4,700 acres in the project area), where it is in fair condition due largely to an overabundance of late succession class with woody understory encroachment.
- California Mixed Evergreen is found over 95% on the Westside, in good condition.
- California Montane Riparian is in fair condition on both sides, with an overabundance of the late succession class.
- California Oak Pine Forest, which is 90% on the Westside, is in fair condition on both sides. It shows as good condition in the North Fork Feather River, due to presence of both early succession and late succession classes, which are scarce elsewhere.
- Curleaf Mountain Mahogany is found exclusively on the Eastside, in fair condition.
- Great Basin Riparian is found 95% on the Eastside, in poor condition, due to over 50% in uncharacteristic native species (Wood's rose, basin big sagebrush, irises), plus no early succession class.
- Lodgepole Pine-Dry shows as poor (just barely) on the Eastside and fair on the Westside. The Eastside condition is due to an overabundance of the open late succession class; however, this may not be problematic, in that LANDFIRE shows this as the dominant class vs. our calculations of NRV based on Sierra climate.
- Lodgepole Pine-Wet shows as fair condition on both sides, due to the same overabundance of the open late succession class.
- Low Sagebrush is found solely on the Eastside, in good condition.
- Mixed Conifer-Mesic Forest is the largest ecosystem and comprises 22% of the project area – over 800,000 acres in the Westside and over 200,000 acres Eastside. It is generally in good

condition, and may have been favored by fire suppression compared to the more fire dependent major forest systems.

- Montane Chaparral is found on both sides, overall in good condition. However, more than any other system, the scores for montane chaparral vary greatly across the ten watersheds. However, like alpine shrubland, this is a very simple ecosystem with only two succession classes. The variances are probably explained by recent fires that temporarily shift large chaparral patches into early succession in some watersheds.
- Montane Sagebrush Steppe is found 98% on the eastside, generally in good condition. The East Branch of the North Fork occurrence, which is actually on the eastside of the project area, is an outlier with an 83% departure score, with almost all of its 35,000 acres in the closed late succession class. Unlike in many areas of the Great Basin with limited conifer seed sources, conifer encroachment is a powerful process in the Sierra Nevada where conifer seed source is abundant. Conifer encroachment is also favored under condition of fire suppression.
- Pinyon-Juniper Woodland is found solely on the Eastside, in good condition.
- Ponderosa Pine – Mixed Conifer is the 3rd largest ecosystem and comprises 16% of the project area – almost 600,000 acres in the Westside and almost 200,000 acres Eastside. It is generally in fair condition, with an overabundance of the closed mid succession class. The good occurrence in the Hone-Eagle Lake watershed is relatively small acreage.
- Red Fir – Western White Pine is abundant and generally in fair condition on both sides.
- Red Fir – White Fir is also abundant and generally in fair condition on both sides due to overabundance of the closed mid-succession class; however, it is in good condition in the Upper Yuba and North Fork American watersheds.
- Subalpine Meadow, the smallest ecosystem (1,300 acres), is in good condition on both sides.
- Subalpine Woodland is generally in good condition on both sides, except for fair condition the Upper Carson and Lake Tahoe watersheds.
- Ultramafic Woodland and Chaparral is found on thin, often serpentine soils, and shows as being in poor condition on both sides, due to an overabundance of the mid succession class. However, this departure score may be explained by the difficulty of remote sensing interpretation of the succession classes for this system.
- Wet Meadow is in poor condition everywhere due to uncharacteristic native species, which exist in different forms. In the Sierra Nevada, lodgepole pine and fir encroachment is common at the edge of wet meadows. This encroachment increases during periods of dry years and fire suppression. Dominance of wet meadows by silver sage, Wood's rose, irises, and big sagebrush is also frequent and a consequence of intense historic grazing or poor current grazing management.

- Yellow Pine is the 2nd largest system in the project area at 890,000 acres, with over 90% located on the eastside. It generally is in fair condition everywhere due to overabundance of the closed mid succession class. Many stands of yellow pine are still young because they are recovering from heavy logging that happened during the mining era of the 19th century.

Appendix D – Ecological Departure Worksheets (Eastside and Westside)

The following worksheets show the departure from the natural range of variability (NRV) for each Northern Sierra biophysical setting/ecological system, by Eastside and Westside. For each system, the tables display the following information by row:

- Name of biophysical setting
- Class: vegetation succession classes (per LANDFIRE model descriptions or Safford adaptations)
- Acres in Class: number of acres currently in each vegetation class, and total acres (last column)
- NRV: NRV percentage in each vegetation class
- Current % in Class: current percentage in each vegetation class
- Ecological Departure: departure from NRV (last column)

Appendix E - Acronyms

BLM	Bureau of Land Management
BpS	Biophysical Settings
BpS refugia	Biophysical Settings refugia
CMIP	Coupled Model Intercomparison Project
CWHR	California Wildlife Habitat Relationships
FRLT	Feather River Land Trust
GCMs	General Circulation Models
IPCC	International Panel on Climate Change
NPS	National Park Service
NRV	Natural range of variability
NSP	Northern Sierra Partnership
PCM	Parallel Climate Model
PCMDI	Program for Climate Model Diagnosis and Intercomparison
PDSI	Palmer Drought Severity Index
PRISM	Parameter-elevation Relationships on Independent Slopes Model
SBC	Sierra Business Council
TDLT	Truckee Donner Land Trust
TNC	The Nature Conservancy
TPL	Trust for Public Land
US EPA	United States Environmental Protection Agency
USFS	United States Forest Service
USGS	United States Geological Survey
VDDT	Vegetation Dynamics Development Tool
WCRP	World Climate Research Programme
WGCM	Working Group on Coupled Modeling